SEMMELWEIS EGYETEM

DOKTORI ISKOLA

Ph.D. értekezések

3347.

TOLVAJ MÁTÉ BALÁZS

Szív-és érrendszeri betegségek élettana és klinikuma

című program

Programvezető: Dr. Merkely Béla, egyetemi tanár

Témavezető: Dr. Kovács Attila, egyetemi docens

RIGHT VENTRICULAR FUNCTION AND PROGNOSIS: MOVING BEYOND CONVENTIONAL ECHOCARDIOGRAPHY

Ph.D. thesis

Máté Balázs Tolvaj, M.D.

Semmelweis University Doctoral School

Cardiovascular Medicine and Research Division

Supervisor: Attila Kovács, M.D., Ph.D.

Official reviewers: Csaba Jenei M.D., Ph.D.
Ádám Tárnoki M.D., Ph.D.

Head of the Complex Examination Committee: Alán Alpár, M.D., D.Sc.

Members of the Complex Examination Committee: László Cervenák, M.D., Ph.D.
Róbert Langer, M.D., Ph.D.

Budapest
2025

TABLE OF CONTENTS

List of abbreviations

2D - two-dimensional

2DE - two-dimensional echocardiography

3D - three-dimensional

3DE - three-dimensional echocardiography

A - late diastolic peak velocity

a′ - mitral annular atrial velocity

ACS - acute coronary syndrome

AIC - Akaike Information Criterion

AMI - acute myocardial infarction

Ap4Ch - apical four-chamber

AUC - area under the curve

BMI - body mass index

BSA - body surface area

CABG - coronary artery bypass grafting

CI - confidence interval

CMR - cardiac magnetic resonance

COPD - chronic obstructive pulmonary disease

CRP - C-reactive protein

CRT-D - cardiac resynchronization therapy with defibrillator

DCM -dilated cardiomyopathy

DT - E-wave deceleration time

E - early diastolic peak velocity

e′ - mitral annular early diastolic velocity

EDA - end-diastolic area

EDV - end-diastolic volume

EDVi - end-diastolic volume index

EF - ejection fraction

ESA - end-systolic area

ESV - end-systolic volume

ESVi - end-systolic volume index

FAC - fractional area change

FWLS - free wall longitudinal strain

GCS - global circumferential strain

GFR - glomerular filtration rate

GLS - global longitudinal strain

HFpEF - heart failure with preserved ejection fraction

HFrEF - heart failure with reduced ejection fraction

HR - hazard ratio

HTX - heart transplantation

ICC - intraclass correlation coefficient

ICD - implantable cardioverter defibrillator

IVSd - interventricular septal thickness at end-diastole

LA - left atrium

LAVi - left atrial volume index

LV- left ventricle

LVAD - left ventricular assist device

LVEF - left ventricular ejection fraction

LVEDVi - left ventricular end-diastolic volume index

LVESVi - left ventricular end-systolic volume index

LVGCS - left ventricular global circumferential strain

LVGLS - left ventricular global longitudinal strain

LVIDd - left ventricular internal diameter at end-diastole

LVIDs - left ventricular internal diameter at end-systole

LVMi - left ventricular mass index

LVSVi - left ventricular stroke volume index

MACE - major adverse cardiovascular event

Mi - mass index

MR - mitral valve regurgitation

PCI - percutaneous coronary intervention

PWd - posterior wall thickness at end-diastole

ROC - receiver-operating characteristic

RV - right ventricle

RVEF - right ventricular ejection fraction

RVEDVi - right ventricular end-diastolic volume index

RVESVi - right ventricular end-systolic volume index

RVGCS - right ventricular global circumferential strain

RVGLS - right ventricular global longitudinal strain

RVSLS – right ventricular septal longitudinal strain

RVSP - right ventricular systolic pressure

RVSVi - right ventricular stroke volume index

s′ - mitral annular systolic velocity

S′ - tricuspid annular systolic velocity

SD - standard deviation

SV - stroke volume

SVi - stroke volume index

TAPSE - tricuspid annular plane systolic excursion

TDI - tissue Doppler imaging

VIF - variance inflation factor

1. Introduction

1.1. The forgotten chamber - historical reappraisal of right ventricular function

The right ventricle (RV) was considered secondary to the left ventricle (LV), primarily serving as a passive conduit between the systemic venous return and the pulmonary circulation for most of the 20th century (1). Its thin-walled structure and seemingly modest contribution to systemic hemodynamics led to a long-standing underestimation of its physiological relevance (2). As a result, the RV was often overlooked in both clinical assessments and scientific research, earning it the retrospective characterization as "the forgotten chamber" (1). This paradigm began to shift in the latter decades of the century, as accumulating clinical and experimental evidence revealed the RV's critical role in maintaining circulatory homeostasis, particularly under conditions of increased afterload such as pulmonary hypertension and left-sided heart failure (3). By the 1990s, advances in imaging techniques and hemodynamic monitoring enabled more precise evaluation of RV structure and function, leading to a renewed interest in right-sided cardiac physiology (4). Before the turn of the millennium, the RV attracted clinical attention, as its complex geometry and distinct pathophysiological responses became recognized as a key component in the progression and prognosis of various cardiovascular diseases (5-7). An increasing volume of research not only challenged the traditional LV-centric model of cardiac function but also positioned the RV as a crucial determinant of patient outcomes in both acute and chronic conditions (8, 9). As such, the once-neglected chamber has become a significant area of focus in cardiovascular research, with RV function now acknowledged as an essential component of comprehensive cardiac assessment (10, 11).

1.2. The importance of right ventricular systolic function in left-sided cardiac diseases

Anatomically and physiologically, the RV differs significantly from the LV (12). Its crescent-shaped geometry, thinner wall, and reliance on longitudinal contraction make it uniquely adapted to its primary role of pumping blood through the low-resistance pulmonary circuit (13). However, these same features render the RV particularly vulnerable to dysfunction in conditions involving pressure overload, volume overload, or myocardial injury (14). RV function not only has prognostic significance in pathologies

primarily affecting the right heart, such as pulmonary hypertension, right-sided heart failure, congenital heart diseases, and chronic obstructive pulmonary disease (COPD), but it has also shown its critical determinant factor of clinical status and prognosis in left-sided heart failure, whether with reduced (HFrEF) or preserved ejection fraction (HFpEF) (15-19). Although the pathophysiology of heart failure is often framed around LV dysfunction, the RV is closely coupled with the LV both anatomically and functionally. This is attributable to the phenomenon of ventricular interdependence, whereby changes in pressure or volume in the LV directly influence the performance of the RV through the shared interventricular septum and pericardial constraint. Additionally, the ventricles exhibit a shared myofiber architecture, particularly in the subepicardial and mid-wall layers, which facilitates coordinated contraction and further links their mechanical performance. In the setting of left-sided heart failure, backward failure can result in elevated pulmonary pressures and subsequent RV pressure overload (20, 21). Numerous studies have demonstrated that RV dysfunction in left-sided heart failure is independently associated with increased mortality, reduced exercise capacity, and higher rates of hospitalization (22, 23). Notably, echocardiographic parameters of RV systolic function offer powerful prognostic information beyond traditional LV metrics, as RV dysfunction signals advanced disease and indicates a worse clinical outcome.

1.3. Conventional echocardiographic parameters of right ventricular systolic function

Conventional echocardiographic parameters for assessing RV systolic function provide critical insights into the mechanics of this structurally and functionally distinct cardiac chamber (11, 24). Among the most widely utilized measures is tricuspid annular plane systolic excursion (TAPSE), which evaluates the longitudinal motion of the lateral tricuspid annulus toward the apex during systole. As the RV contracts predominantly in the longitudinal axis, TAPSE serves as a reliable surrogate for global RV performance, especially in conditions with preserved radial function (25). However, TAPSE is angle- and load-dependent, reflects only regional longitudinal motion, and may underestimate dysfunction in diseases with segmental wall abnormalities or altered RV geometry (26).
RV fractional area change (FAC), which represents the percentage change in RV cavity area between diastole and systole in the apical four-chamber view, provides a two-

dimensional (2D) estimate of global systolic function. While FAC captures both longitudinal and radial components of contraction, its accuracy is limited by the complex, crescent-shaped geometry of the RV, which cannot be fully appreciated in a single 2D plane. Additionally, image quality and inter-observer variability can significantly affect measurement reliability (24, 27).

Tissue Doppler imaging (TDI) of the tricuspid annular systolic velocity (S′) offers another accessible index of RV systolic function, reflecting the peak velocity of the lateral annulus during systole. Though reproducible and easy to obtain, S′ is influenced by preload and afterload, shares TAPSE's regional bias, and may not reflect global RV performance in certain pathologies (28).

RV free wall longitudinal strain (FWLS), derived from 2D speckle-tracking echocardiography, provides a sensitive, angle-independent measure of myocardial deformation along the longitudinal axis (29). FWLS has demonstrated superior prognostic value in numerous conditions and can detect subclinical RV dysfunction before conventional measures are affected. Nevertheless, it requires adequate image quality, is subject to vendor-specific variability, and currently lacks universally standardized cut-off values across platforms, which may limit its widespread applicability and reduce comparability between studies (30, 31).

Despite these limitations, TAPSE, FAC, S′, and FWLS remain the most widely used parameters, when interpreted together and in a clinical context, provide a robust foundation for the evaluation of RV systolic function (Figure 1) (32). Their relative ease of use, prognostic relevance, and integration into international guidelines ensure their continued importance, while also highlighting the need for further refinement through advanced imaging modalities such as three-dimensional echocardiography (3DE), which offers more comprehensive RV assessment and is well validated against cardiac magnetic resonance imaging (CMR) (33-35).

1.4. Three-dimensional echocardiography in right ventricular function assessment

3DE has revolutionized the assessment of RV systolic function by providing detailed and accurate volumetric data (11, 24, 26). Unlike traditional two-dimensional echocardiographic (2DE) methods, which rely on geometric assumptions and limited imaging planes, 3DE captures the RV's complex, crescentic geometry in its entirety.

Image acquisition typically involves a full-volume and electrocardiogram-gated apical four-chamber view using a matrix-array transducer, ensuring that the entire RV cavity is enclosed within the dataset. Post-processing is performed using dedicated software platforms — often with semi-automated border detection — that allow for direct measurement of RV end-diastolic volume (EDV), end-systolic volume (ESV), stroke volume (SV), and right ventricular ejection fraction (RVEF), without the need for geometric extrapolation (Figure 1) (36). The integration of advanced imaging software and increasingly automated analysis workflows enhances reproducibility, which is particularly valuable in longitudinal follow-up, clinical trials, and therapeutic monitoring.

1.5. Three-dimensional motion decomposition of right ventricular function

Recent advances in 3DE have enabled more detailed assessment of RV mechanics beyond global volume and ejection fraction (EF), with particular attention to the directional components of myocardial motion. The ReVISION method (Right VEntrIcular Separate wall motION quantification) is a novel three-dimensional (3D) motion decomposition technique designed to dissect RV systolic function into its three principal components: longitudinal, radial, and anteroposterior contraction (37). The software utilizes a mesh model of the RV and computes directional deformation relative to the center of the cavity, thereby enabling the isolation and quantification of the specific motion vectors contributing to global RV ejection.

By decomposing motion in this way, ReVISION provides a more physiologically relevant understanding of how different myocardial contractions contribute to RV pump function. It allows for measurement of mechanical parameters along the three axes of motion and also global strain metrics, such as right ventricular global longitudinal strain (RVGLS) and right ventricular global circumferential strain (RVGCS) (38). This offers a nuanced appreciation of RV mechanics and can help identify subclinical or regional dysfunction not captured by conventional global indices. ReVISION represents a significant step toward mechanistic, component-based assessment of RV function, enabling a deeper understanding of RV pathophysiology (Figure 1).

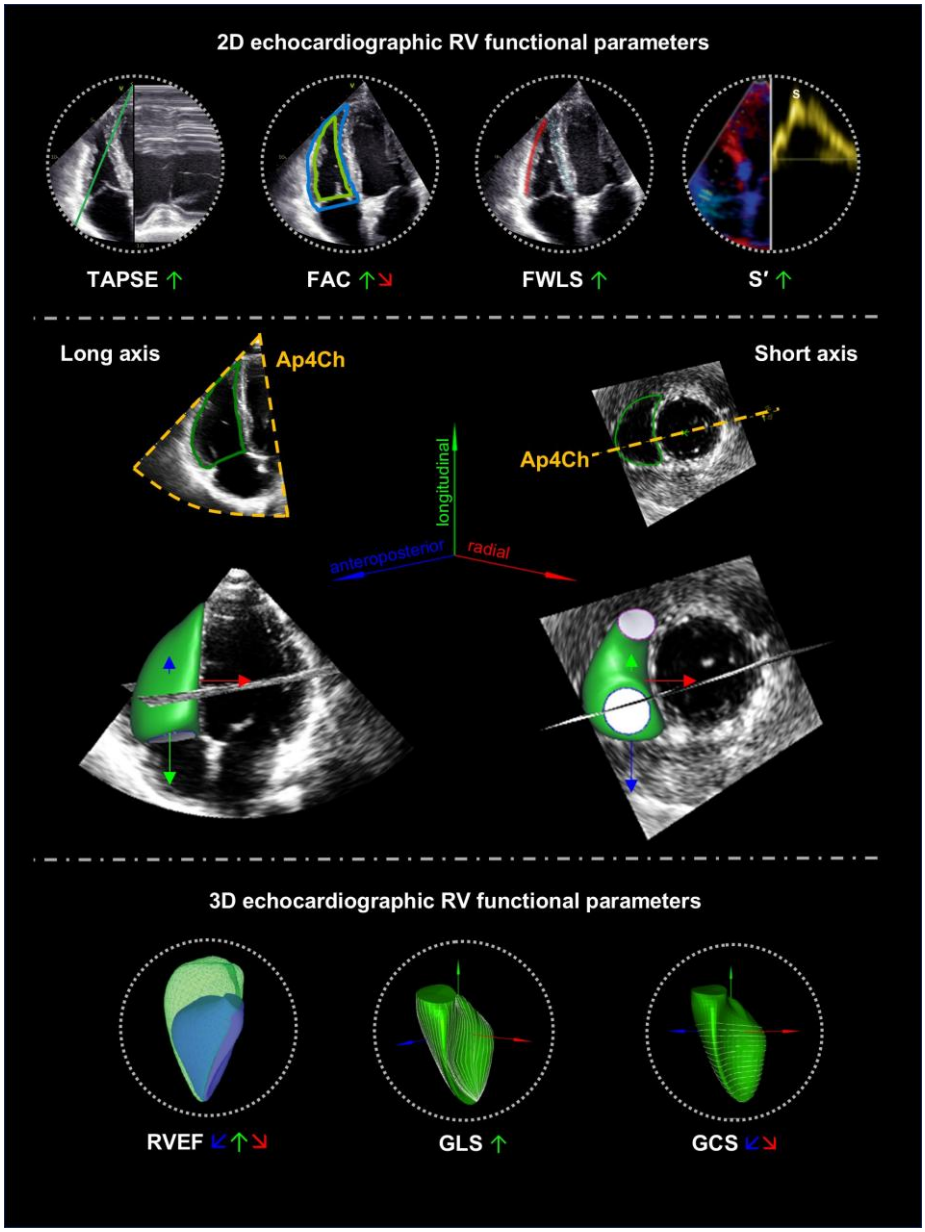

Figure 1. *Illustration of the complex 3D nature of RV structure and mechanics, and the limitations of 2D assessment.*

Upper panel: The most commonly used 2D RV functional parameters derived from the apical four-chamber (Ap4Ch) view are depicted. TAPSE, FWLS, and S′ by TDI reflect only longitudinal shortening, whereas FAC also captures radial shortening.

Middle panel: A 3D RV model is shown within long-axis and short-axis 2D views. The orange lines represent the Ap4Ch view, highlighting its limited depiction of the complex 3D structure. The three principal directions of RV mechanics are illustrated: longitudinal (green arrows), radial (red arrows), and anteroposterior (blue arrows).

Lower panel: 3D RV functional parameters are illustrated. RVEF provides a global measure of RV function, integrating all three directions. RVGLS reflects longitudinal shortening in 3D, while RVGCS captures radial and anteroposterior shortening (Own work, not published earlier).

2. Objectives

2.1. Investigating the added predictive value of right ventricular ejection fraction compared with conventional echocardiographic measurements in patients who underwent diverse cardiovascular procedures

Recently, 3DE-derived RVEF has gained significant scientific interest, as it appears to provide independent prognostic value beyond left ventricular ejection fraction (LVEF) measurements (39). Accordingly, we aimed to investigate the association between RVEF and 2-year all-cause mortality in a diverse population of patients who underwent various cardiovascular procedures at a tertiary care center, and evaluate whether RVEF outperforms conventional echocardiographic parameters in predicting outcomes.

2.2. Evaluating the disagreement between conventional parameters and 3D echocardiography-derived ejection fraction in the detection of right ventricular systolic dysfunction and its association with outcomes

Conventional echocardiographic parameters, such as TAPSE, FAC, and offer only a partial depiction of the complex functional attributes of the RV, whereas 3DE-derived RVEF offers a more comprehensive and integrative evaluation of RV performance. Understanding the divergence in RV systolic function classification by different approaches may substantially influence clinical decision-making, risk stratification, and prognostication. Accordingly, we sought to explore the discordance between TAPSE, FAC, FWLS, and RVEF in the evaluation of RV systolic function and its impact on clinical outcomes.

2.3. Assessing the prognostic significance of RV circumferential strain

The advantages of 3DE over conventional echocardiography facilitate a more comprehensive characterization and quantification of ventricular structure and function, including the assessment of global longitudinal strain (GLS) and global circumferential strain (GCS) for both the LV and RV. Although detailed evaluation of RV function is frequently overlooked in the context of left-sided heart diseases, the presence of RV dysfunction is associated with greater symptom burden and an elevated risk of long-term adverse outcomes. Accordingly, we aimed to evaluate LV and RV GLS and GCS using 3DE in order to determine their prognostic significance.

3. Methods

3.1. Study designs, populations and outcomes

3.1.1. Investigating the added predictive value of right ventricular ejection fraction compared with conventional echocardiographic measurements in patients who underwent diverse cardiovascular procedures

Clinically and hemodynamically stable patients who underwent clinically indicated transthoracic echocardiography at the Heart and Vascular Center of Semmelweis University, Budapest, Hungary, between May 2015 and May 2019 were retrospectively identified. Inclusion criteria were: (1) age ≥18 years; (2) established left-sided cardiac disease with previous or planned cardiac intervention or surgery, regardless of LVEF and RVEF values; (3) availability of 3DE images suitable for 3D LV and RV quantification; and (4) accessible two-year follow-up data. Patients were excluded if they had (1) primary RV pathology (e.g., primary pulmonary hypertension, arrhythmogenic cardiomyopathy, or congenital right heart disease); (2) acute cardiovascular conditions (acute coronary syndrome [ACS], myocarditis, pulmonary embolism, etc.); or (3) inadequate echocardiographic image quality. Clinical characteristics, including demographic data, medical history, physical status and vital signs, as well as laboratory parameters, were retrospectively retrieved from electronic medical records. The study protocol follows the Declaration of Helsinki, and it was approved by the Semmelweis University Regional and Institutional Committee of Science and Research Ethics (approval No. 190/2020). Follow-up data (status [dead or alive], date of death) were obtained from Hungary's National Health Insurance Database. The primary endpoint was all-cause mortality at two years.

3.1.2. Evaluating the disagreement between conventional parameters and 3D echocardiography-derived ejection fraction in the detection of right ventricular systolic dysfunction and its association with outcomes

Patients with various cardiac pathologies who underwent clinically indicated 2DE and 3DE between December 2014 and March 2021 at the Department of Cardiology, Istituto Auxologico Italiano, IRCCS, Milan, Italy, and at the Heart and Vascular Center of Semmelweis University, Budapest, Hungary, were retrospectively identified.

The inclusion criteria comprised: (1) availability of both LV and RV full-volume datasets; (2) adequate image quality and volume rate enabling comprehensive LV and RV volumetric analysis; and (3) availability of follow-up data. All patients underwent standardized 2DE and 3DE imaging protocols. Image quality was assessed subjectively, based on optimization of the pyramidal dataset for width and depth, signal-to-noise ratio, volume rate (ideally ≥20 volumes per second), and the completeness of LV and RV endocardial visualization, and subsequently graded on a scale from 1 (poor) to 5 (excellent). Poor-quality 3DE datasets were considered to have insufficient image quality and were not included in further analyses. Demographic and clinical characteristics, including age, weight, height, body surface area (BSA), body mass index (BMI), systolic and diastolic blood pressure, heart rate, cardiovascular risk factors, comorbidities, and medical history, were extracted from the electronic clinical records. RV systolic dysfunction was defined as RVEF<45%. Guideline-recommended thresholds were applied to identify RV systolic dysfunction using conventional parameters (i.e., TAPSE <17 mm, FAC <35%, and FWLS >−20%). Written informed consent was waived due to the retrospective nature of the study. The study protocol follows the Declaration of Helsinki, and it was approved by the Semmelweis University Regional and Institutional Committee of Science and Research Ethics (approval no. 190/2020) and by the Ethics Committee of the Istituto Auxologico Italiano (approval no. 2021_05_18_13). Follow-up data (status [dead or alive], date of death) were obtained from clinical records, Hungary's National Health Insurance Database, and Italy's National Health Service Database. The primary endpoint of our study was all-cause mortality.

3.1.3. Assessing the prognostic significance of RV circumferential strain

Clinically and hemodynamically stable patients with an established diagnosis of left-sided cardiac disease were selected from the previously published RVENet dataset (https://rvenet.github.io/dataset/) (40). This dataset includes individuals who underwent clinically indicated 2DE and 3DE at the Heart and Vascular Center of Semmelweis University, Budapest, Hungary, between November 2013 and March 2021. Exclusion criteria included: (1) suspicion or presence of any primary right-sided cardiac disease at the initial report or identified during the review of the previously acquired datasets, and (2) suboptimal 3D image quality of the LV and RV datasets precluding accurate 3D

analysis. Demographic and clinical data, including age, weight, height, BSA, BMI, systolic and diastolic blood pressure, heart rate, cardiovascular risk factors, comorbidities, medical history, and laboratory parameters, were obtained from electronic clinical records. Due to the retrospective nature of this analysis, obtaining written informed consent was waived. The study protocol follows the Declaration of Helsinki, and it was approved by the Semmelweis University Regional and Institutional Committee of Science and Research Ethics (approval No. 190/2020). Patients were followed for up to 6 years. Follow-up data (status [dead or alive], date of death) were obtained from Hungary's National Health Insurance Database. The primary endpoint of our study was all-cause mortality.

3.2. Two- and three-dimensional echocardiography

Transthoracic echocardiographic examinations were performed using commercially available ultrasound systems (E9 and E95 with 4V-D or 4Vc-D probes, GE Vingmed Ultrasound, Horten, Norway; and EPIQ 7 with X5-1 probe, Philips Medical Systems, Best, the Netherlands). A standardized acquisition protocol was employed, incorporating 2D loops obtained from parasternal, apical, and subxiphoid views. Digitally stored raw data sets were analyzed offline using dedicated software packages (EchoPAC BT12, GE Vingmed, Horten, Norway; and TomTec Imaging, Unterschleissheim, Germany). Measurements included LV internal diameters, wall thicknesses, relative wall thickness, and mass; left atrial (LA) 2D ESV; mitral inflow velocities such as early diastolic peak velocity (E) and late diastolic peak velocity (A), their ratio, and E wave deceleration time (DT); systolic (s′), early diastolic (e′), and atrial (a′) mitral lateral and septal annular velocities; average E/e′; RV basal short-axis diameter, TAPSE, RV end-diastolic area (EDA) and end-systolic area (ESA), FAC, and right ventricular systolic pressure (RVSP). All parameters were assessed in accordance with current guideline recommendations (24).

In addition to the conventional echocardiographic assessment, electrocardiogram-gated full-volume 3D datasets reconstructed from four or six cardiac cycles and optimized for either the left or right heart were acquired for further analysis on a separate workstation. 3D datasets focused on the left heart were analyzed using semiautomated, commercially

available software (AutoLVQ, EchoPAC BT12, GE Vingmed, Horten, Norway; and 4D LV-Analysis 3, TomTec Imaging, Unterschleissheim, Germany). The following parameters were determined: left ventricular end-diastolic volume index (LVEDVi), left ventricular end-systolic volume index (LVESVi), left ventricular stroke volume index (LVSVi), and left ventricular mass index (LVMi). To evaluate global LV function, LVEF, 3D left ventricular global longitudinal strain (LVGLS), and 3D left ventricular global circumferential strain (LVGCS) were calculated. Concerning the right heart, we quantified 3D right ventricular end-diastolic volume index (RVEDVi), right ventricular end-systolic volume index (RVESVi), right ventricular stroke volume index (RVSVi), RVEF, and 2D FWLS as well (4D RV-Function 2, TomTec Imaging). Additionally, 3D RVGLS and RVGCS were quantified with the ReVISION software (Argus Cognitive, Inc., Lebanon, NH, USA). As previously described, RVGLS is derived by constructing 45 evenly spaced geodesic contours that extend from the RV apex to the base, passing through mid-ventricular points (38). These contours represent the longitudinal shortening of the RV. RVGLS is calculated by measuring the change in length of each contour between end-diastole and end-systole and averaging the results across all contours. For RVGCS, 15 circumferential contours are generated by slicing the RV mesh horizontally at equal intervals along its longitudinal axis, excluding the inflow and outflow tracts. The perimeter of each contour is measured at end-diastole and end-systole, and the average relative change reflects the degree of circumferential shortening (38). By convention, GLS and GCS values are negative; thus, less negative values indicate more impaired ventricular function.

3.3. Statistical analysis

Statistical analyses were conducted using SPSS (versions 22 and 25, IBM, Armonk, NY, USA), GraphPad Prism (version 9.5.1, GraphPad Software, Inc., Boston, MA, USA), and R (version 3.6.2, R Foundation for Statistical Computing, Vienna, Austria). Continuous variables are presented as mean ± standard deviation (SD) or as median with interquartile range, while categorical variables are expressed as frequencies and percentages. Normality of distribution was assessed using the Kolmogorov-Smirnov and Shapiro-Wilk tests. Clinical and echocardiographic characteristics were compared using unpaired Student's t-test or Mann-Whitney U-test for continuous variables, and Chi-squared or

Fisher's exact test for categorical variables, as appropriate. For comparisons involving more than two groups, one-way ANOVA, Welch's ANOVA, or Kruskal-Wallis tests were applied for continuous variables, and χ^2 or Fisher's exact tests for categorical variables. Univariable Cox regression analysis was employed to identify factors associated with all-cause mortality. Multivariable Cox proportional hazards models were constructed and evaluated using the Akaike Information Criterion (AIC) to determine the optimal model fit. Collinearity was assessed using the variance inflation factor (VIF), with a VIF >3 considered indicative of excessive collinearity. Survival curves were generated using the Kaplan-Meier method and compared via log-rank tests. Cox proportional hazards models were used to estimate hazard ratios (HRs) with corresponding 95% confidence intervals (95% CIs) between groups. To assess the prognostic performance of individual echocardiographic parameters, Harrell's C-indices (concordance indices) were compared in univariable Cox models. Receiver-operating characteristic (ROC) curves were constructed to evaluate the discriminative capacity of different echocardiographic parameters, with optimal cut-off values determined using Youden's index. Comparisons of the areas under the ROC curves (AUCs) were performed using the DeLong test (MedCalc Statistical Software, version 22.018, MedCalc Software Ltd, Ostend, Belgium). Sankey diagrams were created using SankeyMATIC (https://sankeymatic.com). Intraobserver and interobserver variability were assessed and reported using intraclass correlation coefficient (ICC) values. A two-sided P-value <0.05 was considered statistically significant.

3.4. Language editing

ChatGPT (version 4o, OpenAI, San Francisco, CA, USA) was used to improve the language of the initial draft of this thesis.

4. Results

4.1. Investigating the added predictive value of right ventricular ejection fraction compared with conventional echocardiographic measurements in patients who underwent diverse cardiovascular procedures

4.1.1. Patient characteristics and outcomes

The study population comprised 174 patients with a mean age of 62 years and a male predominance (72%). Among them, 78 patients (45%) had HFrEF, of whom 69 were referred to our electrophysiology department for evaluation of potential de novo device implantation or device upgrade. During follow-up, 14 patients received an implantable cardioverter defibrillator (ICD), while 49 underwent cardiac resynchronization therapy with defibrillator (CRT-D) implantation. Additionally, 9 patients were assessed for candidacy for LV assist device (LVAD) implantation; subsequently, all received the device. Twenty-eight patients (16%) were heart transplant (HTX) recipients, evaluated at a median of 96 days post-transplantation (range: 9–515 days). Sixty-eight patients (39%) presented with severe primary mitral valve regurgitation (MR; 29 with Barlow's disease and 39 with fibroelastic deficiency), enrolled in a previous prospective study, and subsequently underwent mitral valve repair or replacement following echocardiographic assessment (41). In this cohort, coronary artery disease status had been previously established and, if necessary, treated accordingly. No patients exhibited moderate or severe valvular stenosis. Over a two-year follow-up, 24 patients met the primary endpoint of all-cause mortality: 16 HFrEF patients (2 with ICD, 10 with CRT-D, and 4 with LVAD), 1 HTX patient, and 7 MR patients. Notably, 2 patients in the LVAD group and 2 in the MR group died in the early postoperative period.

4.1.2. Patients meeting vs. not meeting the endpoint

Patients who reached the primary endpoint were compared with those who did not, as summarized in Table 1. Patients who died were older (68 ± 10 years); however, there were no significant differences in anthropometric parameters, blood pressure values, or serum creatinine levels at the time of echocardiographic assessment. Similarly, no differences were observed regarding medical history: the prevalence of coronary artery disease, arterial hypertension, diabetes mellitus, and atrial fibrillation was comparable

between the groups. The presence of significant valvular regurgitations (defined as moderate or severe) was also similar.

Table 1. Baseline clinical and echocardiographic characteristics of the study population

	All (n = 174)	Alive (n = 150)	Dead (n = 24)	p
Demographics, anthropometrics, medical history				
Age (years)	62.3 ± 13.5	61.4 ± 13.7	68.1 ± 10.4	**0.026**
Male, n (%)	126 (72.4)	108 (72.0)	18 (75.0)	0.953
Height (cm)	173.4 ± 12.2	173.6 ± 12.4	171.9 ± 11.1	0.867
Weight (kg)	79.2 ± 15.7	78.8 ± 14.8	82.5 ± 20.7	0.796
BSA (m^2)	1.9 ± 0.2	1.9 ± 0.2	2.0 ± 0.3	0.700
Systolic blood pressure (mmHg)	126.2 ± 19.7	127.5 ± 18.6	118.9 ± 24.9	0.460
Diastolic blood pressure (mmHg)	74.7 ± 16.5	75.3 ± 17.3	71.1 ± 11.5	0.353
Risk factors and medical history				
Diabetes, n (%)	39 (22.5)	33 (22.0)	6 (26.1)	0.866
Hypertension, n (%)	113 (65.3)	98 (65.3)	15 (65.2)	1.000
Coronary artery disease, n (%)	38 (22.0)	33 (22.0)	5 (21.7)	1.000
History or present atrial fibrillation, n (%)	60 (34.7)	52 (34.7)	8 (34.8)	1.000
Moderate or severe mitral regurgitation, n (%)	82 (47.1)	70 (46.7)	12 (50.0)	0.933
Moderate or severe tricuspid regurgitation, n (%)	21 (12.1)	16 (10.7)	5 (20.8)	0.279
Echocardiographic parameters				
LVEDVi (ml/m^2)	94.8 ± 32.6	93.7 ± 32.7	102.6 ± 30.9	0.139
LVESVi (ml/m^2)	52.3 ± 30.5	50.6 ± 30.3	64.0 ± 30.0	**0.026**
LVSVi (ml/m^2)	42.6 ± 19.2	43.1 ± 19.6	38.6 ± 16.3	0.348
LVEF (%)	47.5 ± 17.5	48.6 ± 17.4	39.6 ± 16.3	**0.009**
LVMi (g/m^2)	113.8 ± 37.0	112.9 ± 36.2	119.8 ± 42.3	0.385
LVGLS (%)	−15.5 ± 7.4	−16.0 ± 7.3	−12.1 ± 7.3	**0.017**
E/A	1.6 ± 0.7	1.6 ± 0.7	1.7 ± 0.8	0.639
Deceleration time (ms)	183.1 ± 67.1	182.5 ± 66.4	186.6 ± 72.9	0.998
Mitral lateral annular e' (cm/s)	10.3 ± 3.5	10.3 ± 3.6	9.9 ± 3.2	0.763
Mitral medial annular e' (cm/s)	7.2 ± 2.8	7.3 ± 2.8	6.1 ± 2.4	0.091
E/e'	12.0 ± 5.5	11.8 ± 5.6	13.1 ± 4.8	0.122
RV basal diameter (mm)	30.5 ± 8.3	30.1 ± 8.1	32.8 ± 9.5	0.160
RVEDVi (ml/m^2)	75.5 ± 25.0	73.8 ± 24.0	85.8 ± 28.7	**0.037**
RVESVi (ml/m^2)	41.1 ± 18.7	39.5 ± 17.3	51.5 ± 24.2	**0.009**
RVSVi (ml/m^2)	34.3 ± 10.8	34.3 ± 11.1	34.4 ± 8.9	0.730
RVEF (%)	46.9 ± 9.0	47.6 ± 8.8	42.2 ± 9.2	**0.005**
TAPSE (mm)	20.2 ± 6.6	20.6 ± 6.8	18.0 ± 4.2	0.118
FAC (%)	41.1 ± 8.7	41.7 ± 8.5	37.6 ± 9.5	**0.037**
FWLS (%)	−23.6 ± 7.0	−24.1 ± 6.9	−20.5 ± 7.1	**0.024**
RVSP (mmHg)	36.5 ± 14.9	36.1 ± 15.0	38.7 ± 14.7	0.313

Continuous variables are presented as means ± SD, categorical variables are reported as frequencies (%). BSA: body surface area, EDVi: end-diastolic volume index; EF: ejection fraction; ESVi: end-systolic volume index; FAC: fractional area change; GLS: global longitudinal strain; LV: left ventricular; Mi: mass index; RV: right ventricular; RVSP: right ventricular systolic pressure; SVi: stroke volume index; TAPSE: tricuspid annular systolic excursion

Regarding conventional and 3D echocardiographic parameters, patients who died had higher LVESVi, as well as lower LVEF and LVGLS. In contrast, LVEDVi, LVSVi, and LVMi were similar between the groups. LV diastolic function parameters, including E/A and E/e′ ratios, also showed no significant differences. Patients with adverse outcomes demonstrated significantly higher RVEDVi and RVESVi, while RVSVi was comparable. Among RV functional parameters, RVEF, FAC, and 2D FWLS were significantly reduced in those who died. Importantly, TAPSE and RVSP did not differ between groups.

4.1.3. Univariable Cox proportional hazards models

In univariable Cox analysis, among left-heart echocardiographic parameters, only LVEF (HR [95% CI]: 0.973 [0.950 – 0.997], $p<0.05$) and LVGLS (HR [95% CI]: 1.075 [1.009 – 1.146], $p<0.05$) were significantly associated with the primary endpoint, whereas LV volumes, LVMi, and diastolic function parameters were not. Regarding right-heart metrics, in addition to RVEDVi, RVESVi, FAC, and 2D FWLS, RVEF (HR [95% CI]: 0.945 [0.908 – 0.984], $p<0.01$) was significantly associated with adverse outcomes, while TAPSE and RVSP showed no association (Table 2).

Table 2. Univariable Cox proportional hazards models concerning the primary endpoint

	HR [95% CI for HR]	p
LVEDVi	1.007 [0.996 – 1.019]	0.226
LVESVi	1.012 [1.000 – 1.023]	0.052
LVSVi	0.987 [0.961 – 1.013]	0.312
LVEF	0.973 [0.950 – 0.997]	**0.026**
LVMi	1.005 [0.994 – 1.015]	0.402
LVGLS	1.075 [1.009 – 1.146]	**0.025**
E/A	1.136 [0.610 – 2.113]	0.688
Mitral lateral annular e'	0.968 [0.849 – 1.104]	0.626
Mitral medial annular e'	0.842 [0.687 – 1.031]	0.096
E/e'	1.030 [0.966 – 1.097]	0.367
RVEDVi	1.017 [1.003 – 1.031]	**0.020**
RVESVi	1.027 [1.010 – 1.045]	**0.002**
RVSVi	1.002 [0.966 – 1.039]	0.931
RVEF	0.945 [0.908 – 0.984]	**0.006**
TAPSE	0.943 [0.884 – 1.007]	0.078
FAC	0.951 [0.907 – 0.996]	**0.032**
FWLS	1.071 [1.010 – 1.135]	**0.021**
RVSP	1.010 [0.986 – 1.035]	0.418

CI: confidence interval; EDVi: end-diastolic volume index; EF: ejection fraction; ESVi: end-systolic volume index; FAC: fractional area change; GLS: global longitudinal strain; HR: hazard ratio; LV: left ventricular; Mi: mass index; RV: right ventricular; RVSP: right ventricular systolic pressure; SVi: stroke volume index; TAPSE: tricuspid annular systolic excursion

4.1.4. Comparison of the discriminatory power by receiver-operator characteristic analysis

Using ROC analysis, we assessed the relative discriminatory power of RV systolic function parameters (TAPSE, FAC, FWLS, RVEF) in predicting the primary endpoint. Among these, RVEF showed the highest AUC (0.679; 95% CI: 0.566–0.791) compared with the other RV functional metrics (Table 3). TAPSE and RVEF were directly compared using their respective ROC curves and by evaluating patient subgroups dichotomized at the calculated optimal cut-off values for each parameter (Figure 2).

Table 3. Receiver-operating characteristic analysis comparing the discriminatory power of right ventricular systolic function parameters concerning the primary endpoint

	AUC [95% CI]	Optimal cut-off	Sensitivity	Specificity
RVEF	0.679 [0.566 – 0.791]	48.2 %	0.57	0.79
TAPSE	0.600 [0.501 – 0.698]	24.0 mm	0.35	0.96
FAC	0.630 [0.495 – 0.766]	34.1 %	0.80	0.52
FWLS	0.643 [0.515 – 0.771]	−19.4 %	0.57	0.75

AUC: area under the curve; CI: confidence interval; FAC: fractional area change; RV: right ventricular; RVEF: right ventricular ejection fraction; TAPSE: tricuspid annular systolic excursion

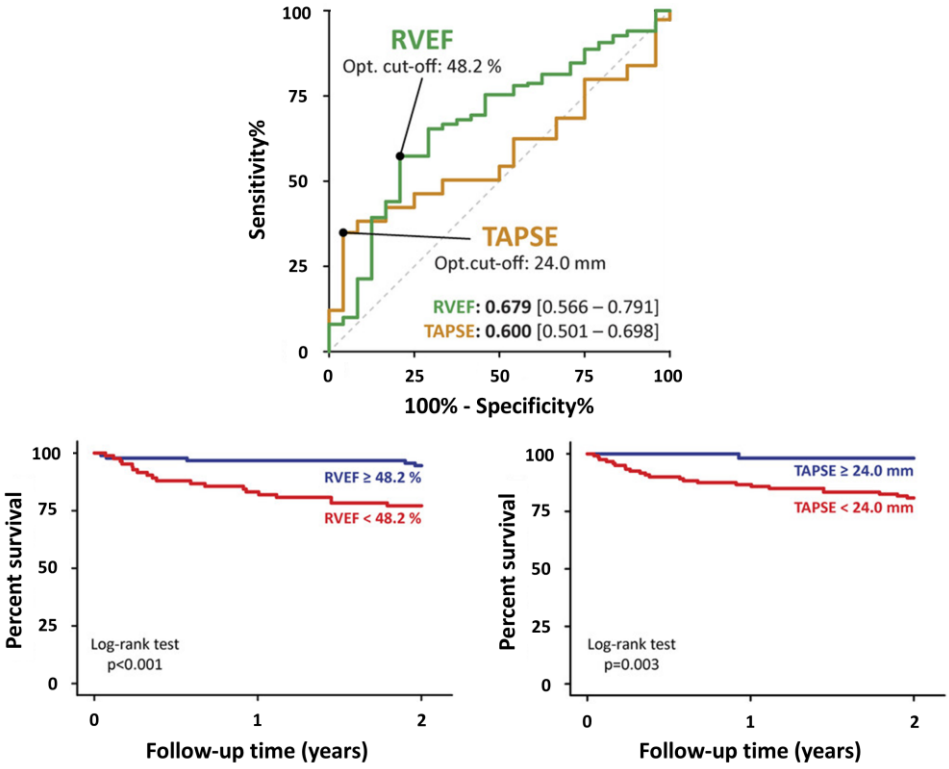

Figure 2. *Comparison of the discriminatory power of TAPSE versus RVEF by ROC analysis concerning the primary endpoint of 2-year all-cause mortality. Outcomes of the patient subgroups dichotomized at the calculated optimal cut-offs of each parameter are visualized on Kaplan-Meier curves (42).*

4.2. Evaluating the disagreement between conventional parameters and 3D echocardiography-derived ejection fraction in the detection of right ventricular systolic dysfunction and its association with outcomes

4.2.1. Patient characteristics and outcomes

In this two-center study, a total of 750 Caucasian patients were included (393 patients from the Department of Cardiology, Istituto Auxologico Italiano, IRCCS, Milan, Italy, and 357 patients from the Heart and Vascular Center, Semmelweis University, Budapest, Hungary). Initially, 906 patients were screened, of whom 156 (17%) were excluded. Exclusion criteria comprised the unavailability of RV or LV 3DE full-volume datasets (42 patients), inadequate 3D image quality for RV or LV analysis (105 patients), irregular rhythm and stitching artifacts (8 patients), and duplication (1 patient). Over a median follow-up period of 3.7 years (interquartile range, 2.7–4.5 years), 112 patients (15%) died.

4.2.2. Patients meeting vs. not meeting the endpoint

Demographic and clinical characteristics of the study cohort, along with a comparison of patients according to outcome, are summarized in Table 4. The most prevalent comorbidities were hypertension (60%), dyslipidemia (46%), coronary artery disease (26%), and diabetes (20%). Patients who died were older, had higher heart rates, a higher prevalence of diabetes and coronary artery disease, and more frequently underwent ICD implantation (Table 4); these conditions and comorbidities were also significant predictors of mortality in univariable Cox regression analysis (Table 5). All assessed 2DE and 3DE parameters of RV size and systolic function differed significantly between patients who stayed alive and those who died during follow-up (Table 4) and were similarly associated with all-cause mortality (Table 5).

Table 4. Demographic and clinical characteristics

	Overall (n=750)	Alive (n=638)	Dead (n=112)	p
Baseline demographic characteristics				
Age (years)	59.4±17.4	58.1±17.3	66.7±15.6	**<0.001**
Male, n (%)	506 (67.5)	432 (67.7)	74 (66.1)	0.733
Height (m)	1.70±0.10	1.71±0.10	1.70±0.10	0.316
Weight (kg)	74.1±15.2	74.2±15.0	73.4±16.2	0.605
BSA (m^2)	1.86±0.23	1.86±0.22	1.84±0.24	0.447
BMI (kg/m^2)	25.4±4.1	25.4±4.0	25.4±4.4	0.936
Systolic blood pressure (mmHg)	123.9±17.9	124.3±17.2	121.5±21.7	0.186
Diastolic blood pressure (mmHg)	74.4±12.5	74.5±12.4	73.8±12.8	0.617
Heart rate (bpm)	72.2±15.9	71.5±15.6	76.3±17.2	**0.025**
Risk factors and medical history				
History of smoking, n (%)	204 (27.2)	173 (27.1)	31 (27.7)	0.902
Diabetes, n (%)	149 (19.9)	113 (17.7)	36 (32.1)	**<0.001**
Dyslipidaemia, n (%)	343 (45.7)	293 (45.9)	50 (44.6)	0.802
Hypertension, n (%)	450 (60.0)	377 (59.1)	73 (65.2)	0.225
ICD, n (%)	76 (10.1)	53 (8.3)	23 (20.5)	**<0.001**
Coronary artery disease, n (%)	200 (26.7)	159 (24.9)	41 (36.6)	**0.010**
Myocardial infarction	159 (21.2)	131 (20.5)	28 (25.0)	0.286
PCI, n (%)	175 (23.3)	143 (22.4)	32 (28.6)	0.155
CABG, n (%)	26 (3.5)	17 (2.7)	9 (8.0)	**0.004**
2D echocardiographic parameters				
RVSP (mmHg)	36.0±17.1	34.0±15.6	47.4±20.9	**<0.001**
TAPSE (mm)	19.8±5.9	20.3±5.9	16.6±5.0	**<0.001**
RVEDAi (cm^2/m^2)	14.4±4.4	14.1±4.2	15.6±5.4	**0.002**
RVESAi (cm^2/m^2)	9.4±3.9	9.1±3.5	11.3±4.9	**<0.001**
FAC (%)	35.4±10.1	36.4±9.7	29.4±10.4	**<0.001**
RVSLS (%)	-13.8±5.5	-14.3±5.4	-11.2±5.7	**0.001**
FWLS (%)	-24.5±6.7	-25.1±6.5	-20.5±6.3	**0.001**
3D echocardiographic parameters				
LVEDVi (ml/m^2)	82.5±31.8	80.3±28.6	94.2±43.9	**<0.001**
LVESVi (ml/m^2)	43.7±29.9	40.9±26.2	59.3±42.2	**<0.001**
LVSVi (ml/m^2)	38.7±13.1	39.4±13.3	34.9±10.8	**<0.001**
LVEF (%)	50.2±14.8	51.5±14.1	42.5±16.4	**<0.001**
RVEDVi (ml/m^2)	80.1±29.7	78.4±28.7	89.4±33.5	**<0.001**
RVESVi (ml/m^2)	43.7±22.6	41.5±20.6	55.9±28.4	**<0.001**
RVSVi (ml/m^2)	36.3±11.6	36.8±11.7	33.5±10.2	**0.006**
RVEF (%)	47.1±9.4	48.3±8.6	40.0±10.5	**<0.001**

Continuous variables are presented as means ± SD, categorical variables are reported as frequencies (%). BMI: body mass index, BSA: body surface area, CABG: coronary artery bypass grafting, EDAi: end-diastolic area index, EDVi: end-diastolic volume index, EF: ejection fraction, ESAi: end-systolic area index, ESVi: end-systolic volume index, FAC: fractional area change, FWLS: free wall longitudinal strain, ICD: implantable cardioverter defibrillator, LV: left ventricle, PCI: percutaneous coronary intervention, RV: right ventricle, RVSLS: right ventricular septal longitudinal strain, RVSP: right ventricular systolic pressure, SVi: stroke volume index, TAPSE: tricuspid annular plane systolic excursion

Table 5. Factors associated with all-cause mortality using univariable Cox regression

	HR [95% CI]	p
Baseline demographic characteristics		
Age	1.040 [1.026 – 1.054]	**<0.001**
Sex (male)	0.861 [0.582 – 1.275]	0.455
Height	0.235 [0.035 – 1.562]	0.134
Weight	0.996 [0.983 – 1.008]	0.495
BSA	0.645 [0.276 – 1.508]	0.311
BMI	1.001 [0.955 – 1.050]	0.961
Systolic blood pressure	0.993 [0.980 – 1.006]	0.280
Diastolic blood pressure	0.992 [0.974 – 1.010]	0.387
Heart rate	1.015 [1.001 – 1.029]	**0.037**
Risk factors and medical history		
History of smoking	1.087 [0.718 – 1.647]	0.693
Diabetes	2.001 [1.343 – 2.982]	**<0.001**
Dyslipidaemia	0.929 [0.639 – 1.350]	0.699
Hypertension	1.273 [0.862 – 1.879]	0.225
ICD	2.676 [1.688 – 4.242]	**<0.001**
Coronary artery disease	1.705 [1.159 – 2.506]	**0.007**
• **Myocardial infarction**	1.264 [0.823 – 1.942]	0.284
• **PCI**	1.367 [0.907 – 2.061]	0.135
• **CABG**	3.018 [1.525 – 5.974]	**0.002**
2D echocardiographic parameters		
RVSP	1.027 [1.019 – 1.035]	**<0.001**
TAPSE	0.911 [0.881 – 0.942]	**<0.001**
RVEDAi	1.061 [1.025 – 1.099]	**<0.001**
RVESAi	1.100 [1.064 – 1.137]	**<0.001**
FAC	0.940 [0.924 – 0.957]	**<0.001**
RVSLS	1.105 [1.067 – 1.144]	**<0.001**
FWLS	1.101 [1.071 – 1.133]	**<0.001**
3D echocardiographic parameters		
LVEDVi	1.011 [1.006 – 1.015]	**<0.001**
LVESVi	1.014 [1.009 – 1.018]	**<0.001**
LVSVi	0.969 [0.952 – 0.987]	**<0.001**
LVEF	0.965 [0.954 – 0.976]	**<0.001**
RVEDVi	1.010 [1.005 – 1.015]	**<0.001**
RVESVi	1.018 [1.013 – 1.024]	**<0.001**
RVSVi	0.972 [0.954 – 0.991]	**0.005**
RVEF	0.928 [0.913 – 0.944]	**<0.001**

CI: confidence interval, HR: hazard ratio. BMI: body mass index, BSA: body surface area, CABG: coronary artery bypass grafting, EDAi: end-diastolic area index, EDVi: end-diastolic volume index, EF: ejection fraction, ESAi: end-systolic area index, ESVi: end-systolic volume index, FAC: fractional area change, FWLS: free wall longitudinal strain, ICD: implantable cardioverter defibrillator, LV: left ventricle, PCI: percutaneous coronary intervention, RV: right ventricle, RVSLS: right ventricular septal longitudinal strain, RVSP: right ventricular systolic pressure, SVi: stroke volume index, TAPSE: tricuspid annular plane systolic excursion

4.2.3. Comparison of right ventricular systolic function parameters

The univariable Cox model including RVEF demonstrated the highest Harrell's C-index (RVEF: 0.729 [95% CI: 0.678 – 0.780], FAC: 0.686 [95% CI: 0.631 – 0.741], FWLS: 0.688 [95% CI: 0.637 – 0.739], TAPSE: 0.664 [95% CI: 0.613 – 0.715]). When comparing the C-indices, RVEF showed significantly superior prognostic power compared to FWLS (p=0.029) and TAPSE (p=0.035), whereas no significant difference was observed compared to FAC (p = 0.130). The HRs of the parameters dichotomized according to guideline-defined cut-off values are presented in Table 6. The greatest increase in the risk of all-cause mortality was identified when RV dysfunction was defined by RVEF (HR [95% CI]: 4.676 [3.169 – 6.900], p<0.001).

Table 6. Hazard ratios of the parameters dichotomized based on the guideline-defined cut-off values

	Univariable Cox proportional-hazards models	
	HR [95% CI]	**p**
RVEF<45%	4.676 [3.169 – 6.900]	**<0.001**
TAPSE<17 mm	2.824 [1.939 – 4.113]	**<0.001**
FAC<35%	3.044 [2.032 – 4.559]	**<0.001**
FWLS>-20%	2.569 [1.767 – 3.736]	**<0.001**

CI: confidence interval, FAC: fractional area change, FWLS: free wall longitudinal strain, HR: hazard ratio, RVEF: right ventricular ejection fraction, TAPSE: tricuspid annular plane systolic excursion

FWLS demonstrated the highest discriminatory power (AUC: 0.877 [95% CI: 0.852 – 0.902, p<0.001]) for identifying RV systolic dysfunction (defined as RVEF<45%), surpassing that of FAC (AUC: 0.787 [95% CI: 0.750 – 0.824, p<0.001]) and TAPSE (AUC: 0.729 [95% CI: 0.690 – 0.767, p<0.001]) (Figure 3). Significant differences were observed among all AUCs based on DeLong tests (FAC vs. FWLS p<0.001; FAC vs. TAPSE p=0.015; FWLS vs. TAPSE p<0.001). According to guideline-recommended cut-off values, the sensitivity and specificity for detecting RV systolic dysfunction (RVEF<45%) were 55% and 79% for TAPSE, 76% and 67% for FAC, and 59% and 92% for FWLS, respectively, as determined by ROC analysis.

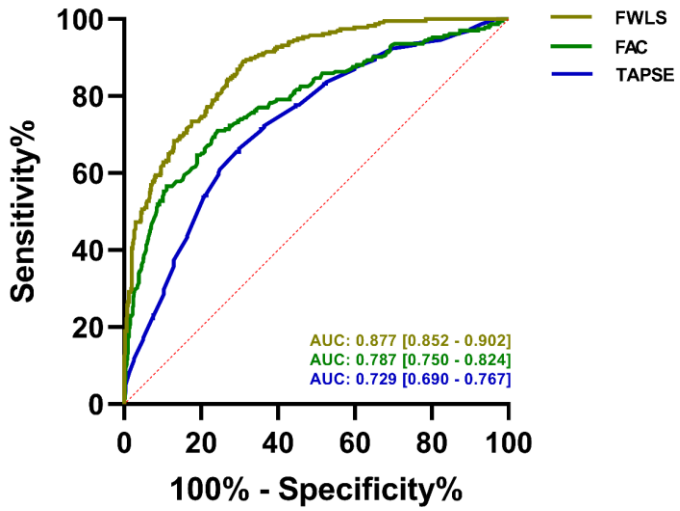

Figure 3. *ROC curves of the conventional parameters for the discrimination of RV systolic dysfunction (RVEF<45%) with corresponding AUC values (43).*

4.2.4. Multiparametric assessment of right ventricular systolic function using conventional parameters

Clinical outcomes were the worst if at least two conventional echocardiographic parameters indicated RV systolic dysfunction, and progressively improved when only one or none of these parameters was abnormal. All Kaplan-Meier curves differed significantly from each other (log-rank p<0.005), except for the comparison between the curves representing two versus three impaired parameters (Figure 4).

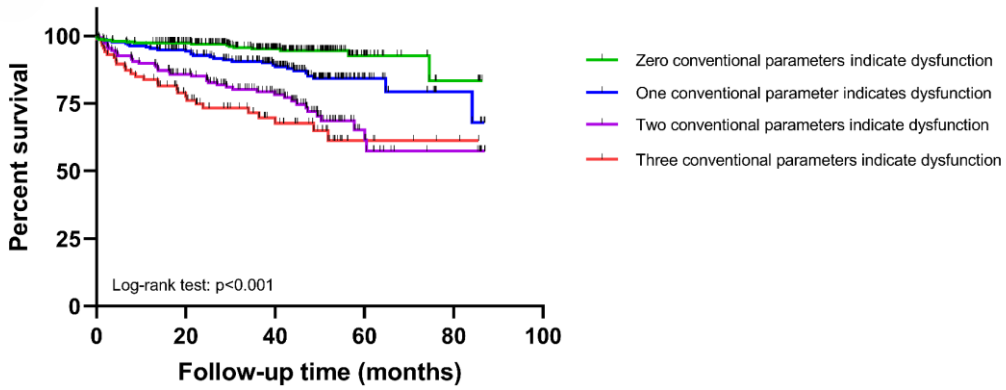

Figure 4. *Survival analysis of patients divided into subgroups based on the number of conventional parameters indicating RV dysfunction. The survival of patients is visualized via Kaplan-Meier curves with the p-value of the overall log-rank test (43).*

HRs for all-cause mortality across subgroups defined by the number of conventional parameters indicating RV dysfunction are summarized in Table 7. The risk of death more than doubled (HR [95% CI]: 2.176 [1.348 – 3.511], p=0.001) when two conventional parameters indicated dysfunction, and nearly tripled (HR [95% CI]: 2.890 [1.707 – 4.891], p<0.001) when three parameters indicated dysfunction, compared with cases in which only one parameter indicated dysfunction.

Table 7. Hazard ratios of all-cause mortality in the different subgroups based on the number of conventional parameters indicating RV dysfunction

Cox proportional-hazards models		
	HR [95% CI]	**p**
Zero vs. One	2.371 [1.286 – 4.373]	**0.006**
Zero vs. Two	5.302 [2.968 – 9.472]	**<0.001**
Zero vs. Three	6.972 [3.749 – 12.963]	**<0.001**
One vs. Two	2.176 [1.348 – 3.511]	**0.001**
One vs. Three	2.890 [1.707 – 4.891]	**<0.001**
Two vs. Three	1.315 [0.806 – 2.145]	0.272

CI: confidence interval, HR: hazard ratio

To identify the most effective pair of conventional parameters for combined assessment, we calculated the HRs for all three possible parameter combinations. The combination of FAC and FWLS indicating RV dysfunction exhibited the highest HR compared to cases with zero parameters indicating dysfunction (HR [95% CI]: 5.841 [2.107 – 16.190], p=0.001; Table 8).

Table 8. Hazard ratios of the subgroups created based on the different combinations of two conventional parameters indicating RV dysfunction

Univariable Cox proportional-hazards models		
	HR [95% CI]	**p**
Zero parameters vs. both FAC and FWLS indicating dysfunction	5.841 [2.107 – 16.193]	**<0.001**
Zero parameters vs. both TAPSE and FAC indicating dysfunction	5.754 [2.510 – 13.150]	**<0.001**
Zero parameters vs. both TAPSE and FWLS indicating dysfunction	2.867 [0.571 – 14.397]	**0.046**
Zero parameters vs. both FAC and FWLS indicating dysfunction	5.841 [2.107 – 16.193]	**<0.001**

CI: confidence interval, FAC: fractional area change, FWLS: free wall longitudinal strain, HR: hazard ratio, TAPSE: tricuspid annular plane systolic excursion

However, log-rank tests showed no significant differences between the Kaplan-Meier curves of any two-parameter combinations and those of the subgroup with all three parameters indicating dysfunction (Figure 5).

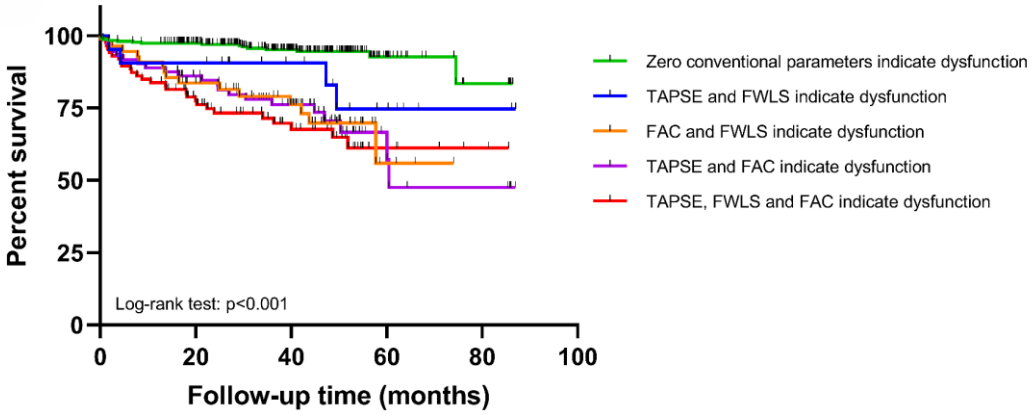

Figure 5. *Survival analysis of patients divided into subgroups based on the two-parameter combinations of conventional parameters indicating RV dysfunction. The survival of patients is visualized via Kaplan-Meier curves with the p-value of the overall log-rank test (43).*

There were also no significant differences between the Kaplan-Meier curves when the subgroups were defined by the presence of RV dysfunction indicated by any two conventional parameters, regardless of the value of the third parameter (Figure 6).

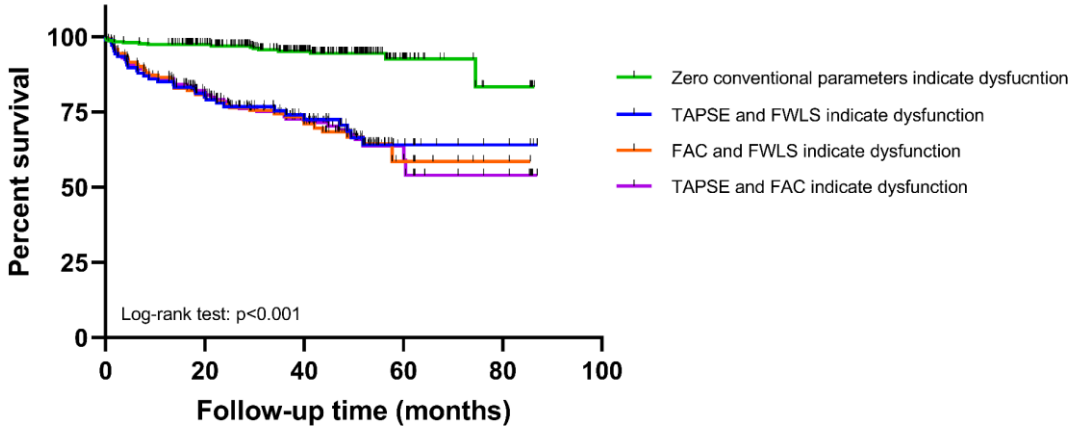

Figure 6. *Survival analysis of patients divided into subgroups by evaluating whether a combination of two conventional parameters indicates RV dysfunction irrespective of the third parameter's value. The survival of patients is visualized via Kaplan-Meier curves with the p-value of the overall log-rank test (43).*

4.2.5. Reclassification of right ventricular systolic function by ejection fraction

4.2.5.1. Reclassification in the full cohort

In total, 511 patients (68%) exhibited normal RV function when assessed by RVEF. Although an equivalent number of patients were classified as having normal RV function using TAPSE, 21% of these demonstrated impaired RVEF. When using FAC, only 404 patients were categorized as having preserved RV function; however, 15% of this subgroup had RV dysfunction according to RVEF. In contrast, FWLS identified 567 patients without dysfunction, yet 17% of these were reclassified as having RV dysfunction based on RVEF (Figure 7).

Conversely, RV dysfunction was identified in 239 patients (32%) based on RVEF. While TAPSE classified an identical number of patients as having dysfunction, 46% of these were misclassified relative to RVEF. Using FAC, 346 patients were assigned to the dysfunction group; however, 49% of these did not exhibit dysfunction according to RVEF. In contrast, FWLS identified 183 patients with RV dysfunction, with 23% subsequently reclassified as having preserved function when evaluated by RVEF (Figure 7).

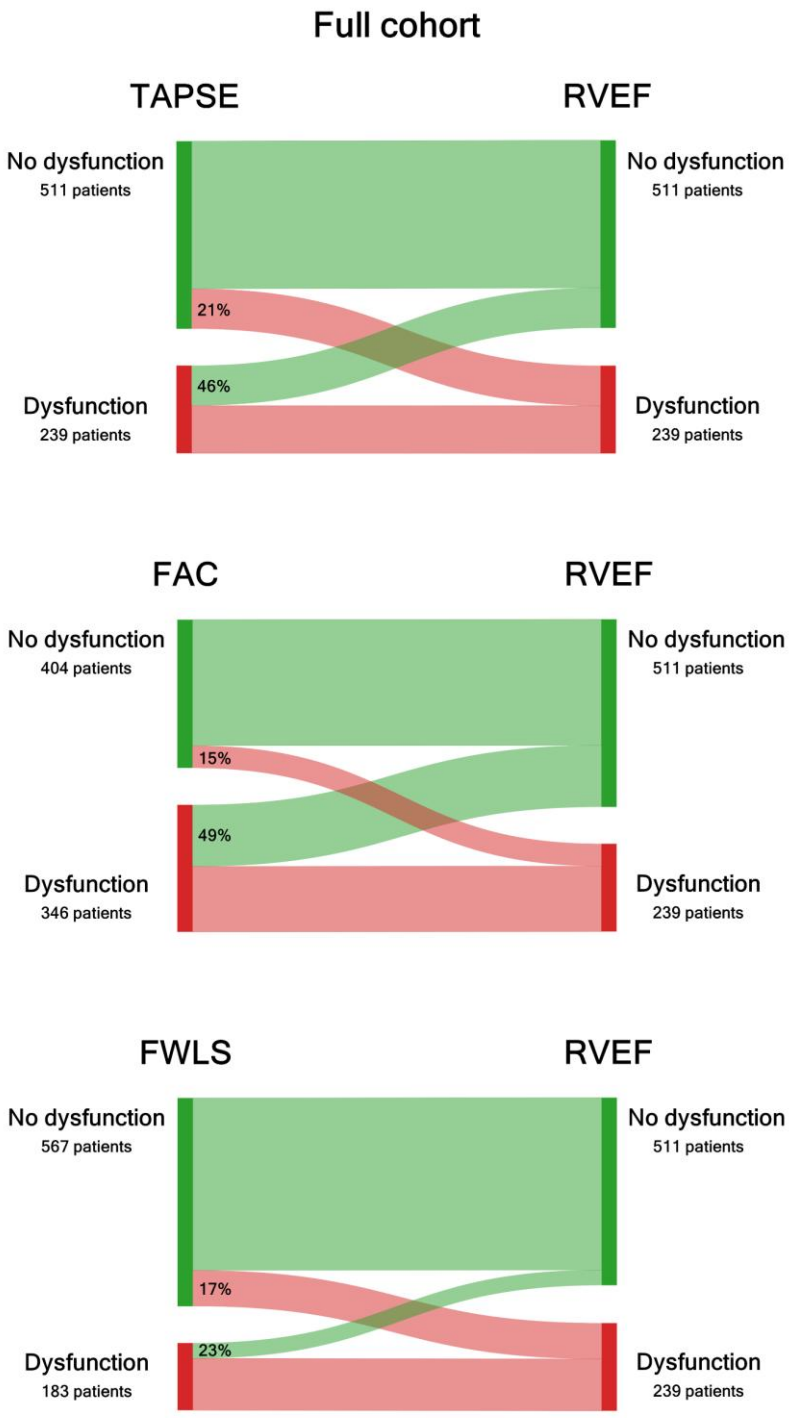

***Figure 7**. Disagreement in the classification of RV systolic function between conventional parameters and 3DE-derived RVEF. To visualize the rate of reclassification occurring in the full cohort by RVEF-based assessment, Sankey diagrams were constructed. Green flows represent patients without RV dysfunction, and red flows represent patients with RV dysfunction by RVEF (43).*

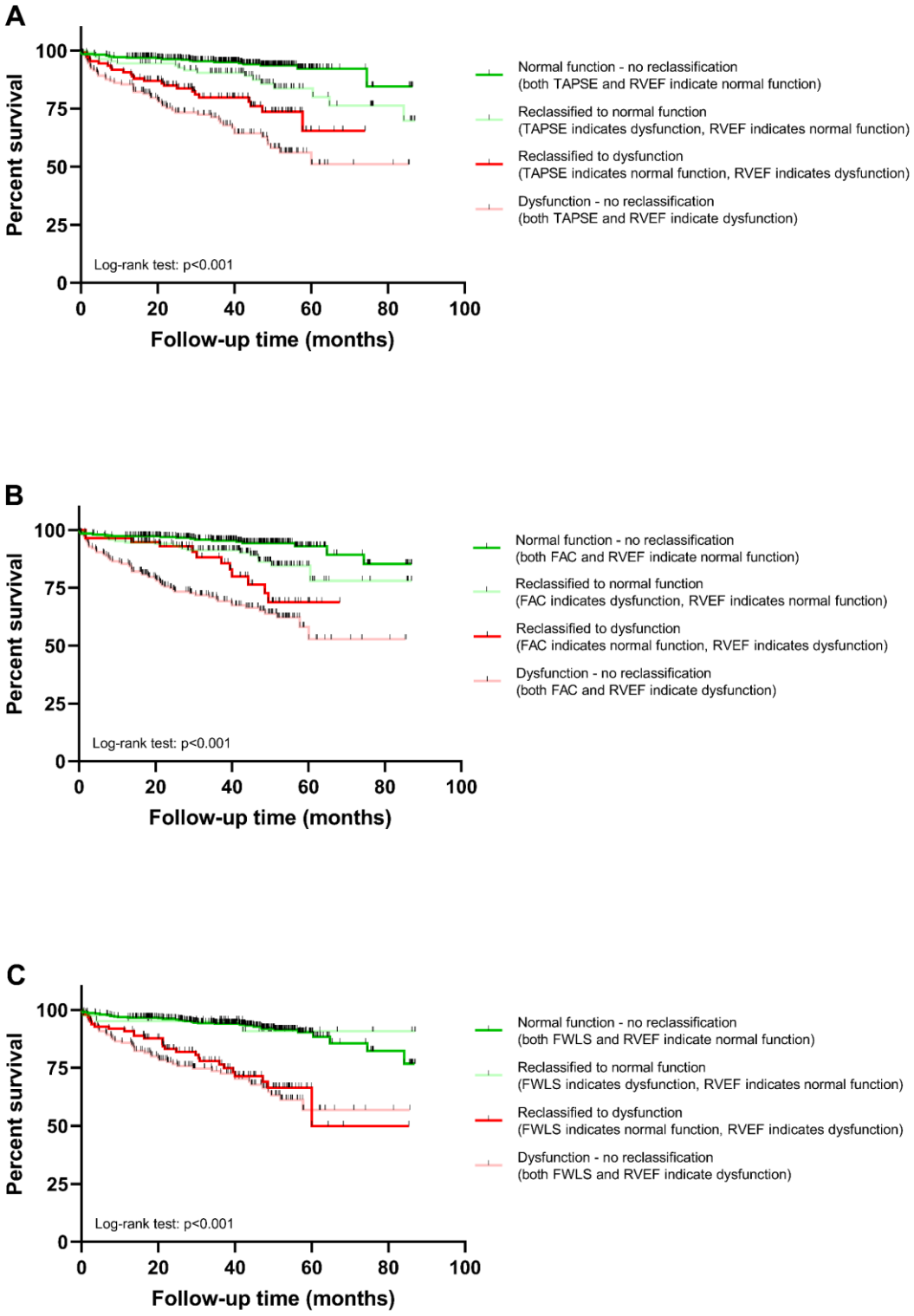

Figure 8. *Survival analysis of patients divided into subgroups based on the combination of different parameters detecting right ventricular systolic dysfunction. The survival of patients is visualized via Kaplan-Meier curves with the p-value of the overall log-rank test. Green and red colors with the same opacity were used to indicate subgroups that were compared due to reclassification based on RVEF (43).*

To further clarify the clinical significance of RVEF-based reclassification, outcomes were compared between reclassified and non-reclassified patients (Figure 8). Patients with normal conventional parameters who were reclassified as having RV dysfunction exhibited a more than four-fold increased risk of mortality compared to those not reclassified (TAPSE HR [95% CI]: 4.395 [2.127 – 9.085], p<0.001; FAC HR [95% CI]: 4.186 [1.476 – 11.880], p<0.001; FWLS HR [95% CI]: 4.221 [2.115 – 8.426], p<0.001). Conversely, patients with abnormal conventional parameters who were reclassified as having normal RV function demonstrated a substantially lower mortality risk relative to non-reclassified patients (TAPSE HR [95% CI]: 0.326 [0.199 – 0.532], p<0.001; FAC HR [95% CI]: 0.308 [0.197 – 0.480], p<0.001; FWLS HR [95% CI]: 0.195 [0.102 – 0.373], p=0.002). Importantly, however, there was an added mortality risk in those subgroups where RVEF was normal, but TAPSE or FAC was abnormal compared to those subgroups in which both RVEF and TAPSE or FAC were within normal ranges (TAPSE HR [95% CI]: 2.111 [1.041 – 4.280] p=0.014, FAC HR [95% CI]: 2.237 [1.142 – 4.384] p=0.010).

4.2.5.2. Subgroup analysis

The study cohort was categorized into the following clinical subgroups: aortic valve disease (n=120, 16%), mitral valve disease (n=108, 14%), HTX (n=91, 12%), non-ischemic dilated cardiomyopathy (DCM) (n=88, 12%), ischemic cardiomyopathy (n=76, 10%), ACS (n=82, 11%), other cardiomyopathy (n=31, 4%) and a heterogeneous subgroup comprising various other cardiac diseases (n=154, 21%).

Regarding the subgroups' classification based on TAPSE, the highest reclassification rate was observed among HTX patients (71%), followed by those with ischemic cardiomyopathy (32%), non-ischemic DCM (31%), aortic valve disease (25%), ACS (21%), and mitral valve disease (17%) (Figure 9).

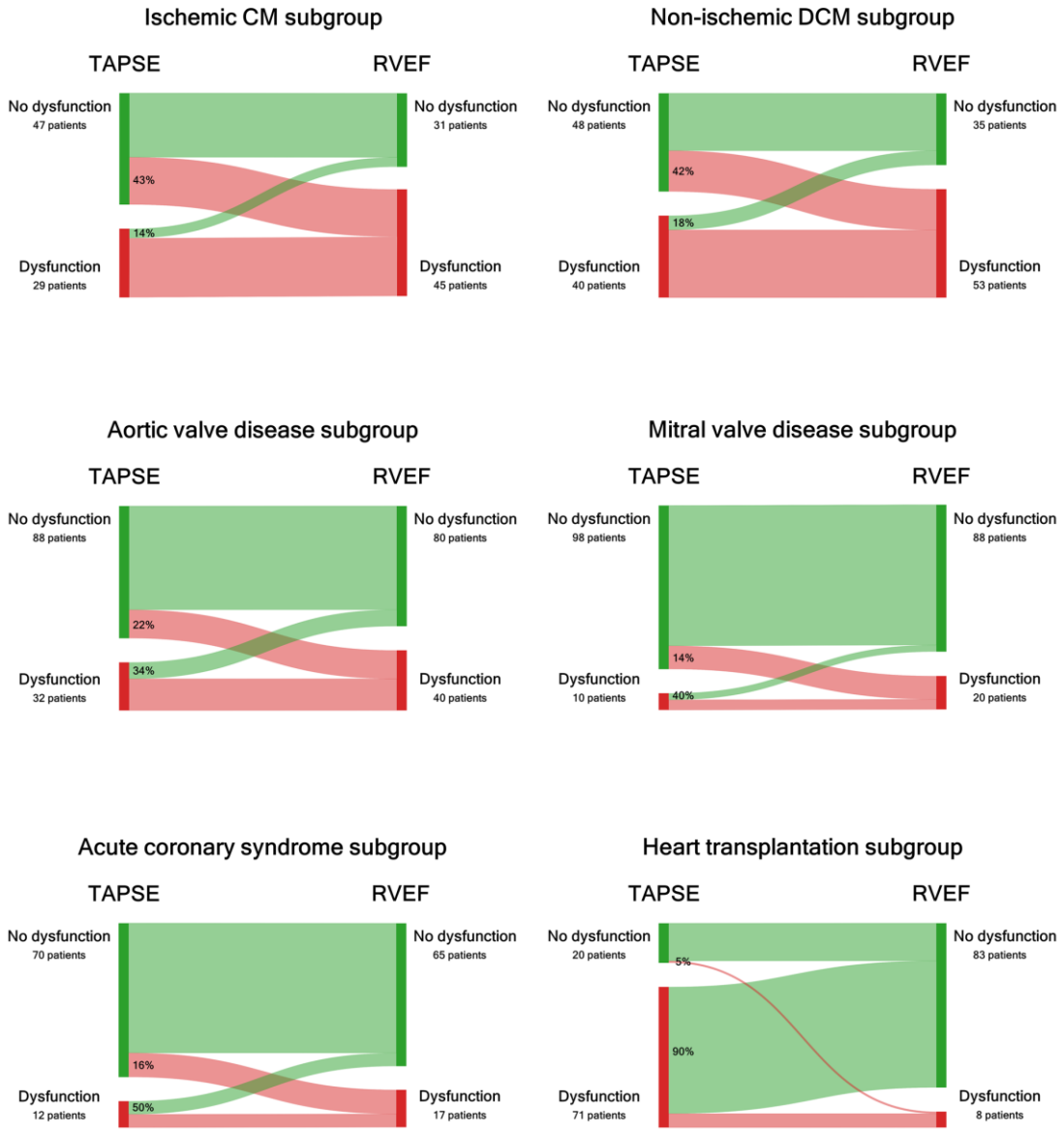

Figure 9. *Detailed breakdown of reclassifications occurring in the different subgroups based on the disagreement between TAPSE and 3DE-derived RVEF, visualized on Sankey diagrams. Green flows represent patients without RV dysfunction, and red flows represent patients with RV dysfunction by RVEF (43).*

When RV function was evaluated using FAC, reclassification was observed in 51% of patients with mitral valve disease, 40% of HTX patients, 30% of those with non-ischemic DCM, 28% with ischemic cardiomyopathy, 25% with aortic valve disease, and 17% with ACS (Figure 10).

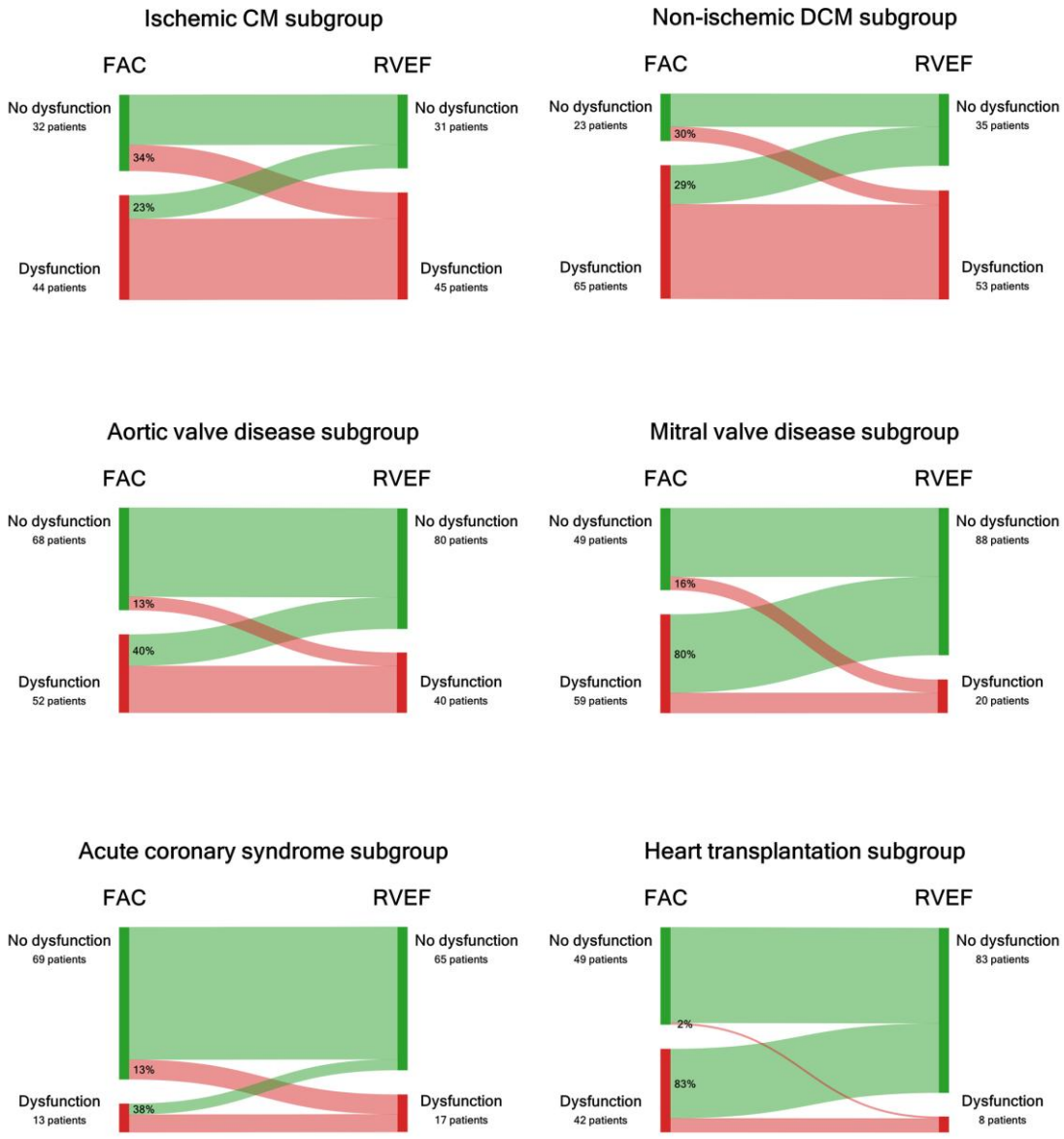

Figure 10. *Detailed breakdown of reclassifications occurring in the different subgroups based on the disagreement between FAC and 3DE-derived RVEF, visualized on Sankey diagrams. Green flows represent patients without RV dysfunction, and red flows represent patients with RV dysfunction by RVEF (43).*

The evaluation based on FWLS demonstrated comparable or lower rates of reclassification relative to other conventional functional parameters. Specifically, reclassification occurred in 28% of patients with ischemic cardiomyopathy, 20% in those with non-ischemic DCM and aortic valve disease, 19% in the HTX subgroup, 17% in the ACS subgroup, and 13% among patients with mitral valve disease. (Figure 11).

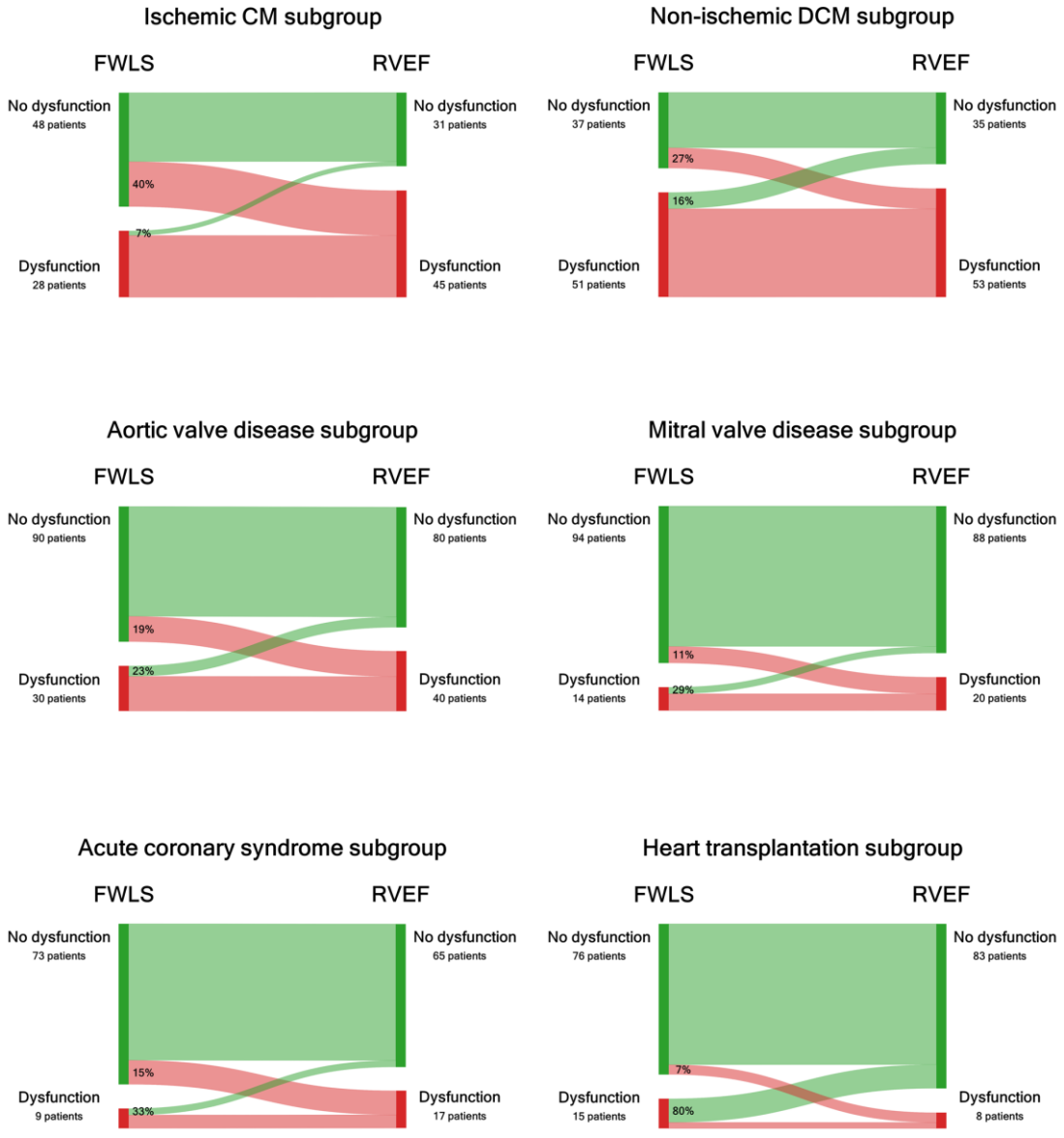

Figure 11. *Detailed breakdown of reclassifications occurring in the different subgroups based on the disagreement between FWLS and 3DE-derived RVEF, visualized on Sankey diagrams. Green flows represent patients without RV dysfunction, and red flows represent patients with RV dysfunction by RVEF (43).*

4.3. Assessing the prognostic significance of RV circumferential strain

4.3.1. Patient characteristics and outcomes

A total of 357 patients (age: 64 ± 15 years, 70% male) with established left-sided cardiac disease and 3DE recordings of suitable quality for both LV and RV analysis were identified from the RVENet dataset. Of the initial 444 patients, 80 were excluded due to inadequate 3D image quality for RV analysis, and an additional 7 due to suboptimal image quality for LV analysis.

Over a median follow-up time of 41 months (interquartile range 20–52), 55 (15%) patients died. The demographic and clinical characteristics of the study population, along with a comparison between patients alive vs. those who died, are presented in Table 9.

Table 9. Demographic and clinical characteristics

	Overall (n=357)	**Alive (n=302)**	**Dead (n=55)**	**p**
Baseline demographic characteristics				
Age (years)	64.2±14.5	63.4±14.6	68.6±13.1	**0.014**
Male, n (%)	249 (69.7)	211 (69.9)	38 (69.1)	0.908
BSA (m^2)	1.93±0.22	1.93±0.22	1.91±0.22	0.494
BMI (kg/m^2)	26.8±4.2	27.0±4.3	26.0±3.6	0.288
Systolic blood pressure (mmHg)	126.5±18.4	126.1±17.2	128.0±23.2	0.585
Diastolic blood pressure (mmHg)	74.6±15.3	74.0±15.9	77.4±12.3	0.230
Heart rate (bpm)	77.6±14.6	77.7±15.0	77.4±12.5	0.935
Risk factors and medical history				
Hypertension, n (%)	260 (72.8)	218 (72.2)	42 (76.4)	0.522
History of smoking, n (%)	82 (23.0)	66 (21.9)	16 (29.1)	0.241
COPD, n (%)	40 (11.2)	33 (10.9)	7 (12.7)	0.735
Diabetes, n (%)	99 (27.7)	78 (25.8)	21 (38.2)	0.060
History of atrial fibrillation, n (%)	116 (32.5)	89 (29.5)	27 (49.1)	**0.005**
Pacemaker, n (%)	49 (13.7)	38 (12.6)	11 (20.0)	0.159
ICD, n (%)	33 (9.2)	23 (7.6)	10 (18.2)	**0.015**
CRT-D, n (%)	15 (4.2)	12 (4.0)	3 (5.5)	0.637
Coronary artery disease, n (%)	77 (21.6)	55 (18.2)	22 (40.0)	**<0.001**
Previous CABG, n (%)	19 (5.3)	13 (4.3)	6 (10.9)	**0.045**
Previous PCI, n (%)	67 (18.8)	49 (16.2)	18 (32.7)	**0.004**
Previous AMI, n (%)	48 (13.4)	34 (11.3)	14 (25.5)	**0.005**
Laboratory parameters				
GFR ($mL/min/1.73m^2$)	61.0±19.4	62.1±19.1	56.3±20.2	0.056
Creatinine (µmol/L)	101.1±41.7	99.1±38.6	112.1±54.5	**0.035**
Hemoglobin (g/dL)	12.9±2.1	12.9±2.1	12.6±2.2	0.385
CRP (mg/L)	6.7±11.9	6.3±12.1	9.0±10.5	0.134

Continuous variables are presented as means ± SD, categorical variables are reported as frequencies (%). AMI: acute myocardial infarction, BMI: body mass index, BSA: body surface area, CABG: coronary artery bypass grafting, COPD: chronic obstructive pulmonary disease, CRP: C-reactive protein, CRT-D: cardiac resynchronization therapy with defibrillator, GFR: glomerular filtration rate, ICD: implantable cardioverter defibrillator, PCI: percutaneous coronary intervention

Ninety-five subjects (27%) were HFrEF patients; among them, 81 were referred to the electrophysiology department for evaluation prior to device implantation (pacemaker/ICD/CRT-D). Fourteen HFrEF patients were assessed for candidacy for LVAD implantation. Ninety-one subjects (26%) were HTX recipients, evaluated at a median of 157 days post-transplantation (ranging from 8 to 6,571 days). Sixty-seven subjects (19%) had severe primary MR and had been enrolled in a previous prospective study (10). Seventy-nine patients (22%) were investigated to assess the severity of aortic stenosis (moderate or severe). Additionally, twenty-five patients (7%) with a history of atrial fibrillation were referred for evaluation prior to potential catheter ablation. The most prevalent comorbidities of the cohort were hypertension (73%), diabetes (28%), coronary artery disease (22%), and atrial fibrillation (33%).

4.3.2. Patients meeting vs. not meeting the endpoint

Patients who died were older, exhibited a higher prevalence of coronary artery disease and atrial fibrillation, and more frequently underwent ICD implantation in their medical history. Moreover, these patients demonstrated significantly elevated serum creatinine levels compared with those who survived (Table 9).

4.3.3. Echocardiographic characteristics

2DE parameters are summarized in Table 10. Interestingly, conventional morphological parameters of the LV, the LA, and the RV did not differ between patients who died vs. those who survived. Mitral annular velocities by TDI, both in systole and diastole, were more impaired in those patients who died. In contrast, the E/e′ ratio did not differ between groups. The right atrial size was larger in those patients who died, accompanied by more pronounced impairment of RV longitudinal function, as reflected by reduced TAPSE and FWLS; however, RVSP and FAC were similar.

Table 10. 2D echocardiographic parameters

	Overall (n=357)	Alive (n=302)	Dead (n=55)	p
2D echocardiographic parameters				
LVIDd (mm)	53.8±9.8	53.5±9.7	55.5±10.0	0.157
LVIDs (mm)	42.0±14.0	41.2±13.8	45.8±14.3	0.073
IVSd (mm)	11.5±2.6	11.6±2.6	11.1±2.6	0.185
PWd (mm)	10.2±2.2	10.2±2.1	10.1±2.8	0.556
LVMi (g/m^2)	120.3±35.8	119.9±36.5	122.5±32.1	0.632
E (cm/s)	98.4±34.2	97.3±32.3	104.4±43.1	0.179
A (cm/s)	72.0±30.8	73.2±30.5	64.1±31.5	0.095
E/A	1.52±0.71	1.50±0.70	1.71±0.79	0.097
DT (ms)	176.6±58.6	177.9±58.9	169.1±56.7	0.379
Mitral lateral s′ (cm/s)	8.4±3.0	8.6±2.9	6.9±2.7	**<0.001**
Mitral lateral e′ (cm/s)	10.5±3.9	10.6±3.9	9.8±3.5	0.186
Mitral lateral a′ (cm/s)	7.9±3.2	8.2±3.3	6.1±2.3	**<0.001**
Mitral medial s′ (cm/s)	6.7±2.3	6.8±2.2	5.7±2.2	**0.003**
Mitral medial e′ (cm/s)	7.2±2.9	7.4±2.9	6.1±2.6	**0.013**
Mitral medial a′ (cm/s)	7.3±2.6	7.4±2.6	6.2±2.6	**0.020**
E/e′ average	12.1±6.4	11.8±6.1	13.6±7.8	0.093
LAVi (ml/m^2)	46.6±19.5	46.4±20.3	48.0±15.1	0.601
RV basal diameter (mm)	35.5±5.9	35.2±5.9	36.9±6.0	0.080
RVSP (mmHg)	40.6±13.8	39.6±13.7	45.1±13.5	0.059
TAPSE (mm)	19.3±6.3	19.7±6.4	17.3±5.2	**0.011**
FAC (%)	42.9±9.2	43.3±9.0	40.9±9.7	0.079
RVSLS (%)	-14.3±6.1	-14.6±6.0	-12.2±6.5	**0.008**
FWLS (%)	-24.0±6.6	-24.5±6.6	-21.4±6.2	**0.002**

Continuous variables are presented as means ± SD, categorical variables are reported as frequencies (%). A: mitral inflow velocity during atrial contraction, a': mitral annular atrial velocity, DT: E-wave deceleration time, E: early diastolic mitral inflow velocity, e': mitral annular early diastolic velocity, FAC: fractional area change, FWLS: free wall longitudinal strain, IVSd: interventricular septal thickness at end-diastole, LAVi: left atrial volume index, LV: left ventricle, LVIDd: LV internal diameter at end-diastole, LVIDs: LV internal diameter at end-systole, Mi: mass index, PWd: posterior wall thickness at end-diastole, RV: right ventricle, RVSLS: right ventricular septal longitudinal strain, RVSP: right ventricular systolic pressure, s': mitral annular systolic velocity, TAPSE: tricuspid annular plane systolic excursion

3DE parameters are summarized in Table 11. Patients who died exhibited larger LV and RV volumes, as well as more severely impaired systolic function. Notably, LVSVi and RVSVi were similar. Regarding longitudinal and circumferential strain parameters, both LV and RV GLS and GCS were more impaired in patients who died.

Table 11. 3D echocardiographic parameters

	Overall (n=357)	Alive (n=302)	Dead (n=55)	p
Left ventricle				
LVEDVi (ml/m²)	82.2±32.2	80.3±32.3	91.9±30.3	**0.019**
LVESVi (ml/m²)	44.5±30.4	42.2±30.0	56.3±30.0	**0.003**
LVSVi (ml/m²)	37.7±14.6	38.1±15.1	35.6±11.2	0.269
LVMi (g/m²)	102.5±36.8	100.4±35.1	113.4±43.0	**0.023**
LVEF (%)	49.0±15.7	50.2±15.3	42.3±16.1	**0.001**
LVGLS (%)	-15.2±6.0	-15.7±5.9	-12.5±6.2	**<0.001**
LVGCS (%)	-23.9±9.1	-24.6±9.0	-20.2±9.3	**0.001**
Right ventricle				
RVEDVi (ml/m²)	70.2±23.5	68.9±23.1	76.6±24.6	**0.033**
RVESVi (ml/m²)	37.4±18.7	36.0±17.8	44.4±21.3	**0.003**
RVSVi (ml/m²)	32.7±9.0	32.8±9.3	32.2±7.5	0.648
RVEF (%)	48.3±9.4	49.1±9.2	44.1±9.5	**<0.001**
RVGLS (%)	-16.4±5.1	-16.9±5.0	-13.8±4.6	**<0.001**
RVGCS (%)	-17.7±6.1	-18.3±5.9	-14.3±6.2	**<0.001**

Continuous variables are presented as means ± SD, categorical variables are reported as frequencies (%). EDVi: end-diastolic volume index, EF: ejection fraction, ESVi: end-systolic volume index, GCS: global circumferential strain, GLS: global longitudinal strain, LV: left ventricle, Mi: mass index, RV: right ventricle, SVi: stroke volume index

4.3.4. Multivariable Cox regression models

Using univariable Cox regression, we identified variables associated with all-cause mortality (44). Subsequently, we constructed multiple multivariable Cox models, each incorporating a maximum of five predictors, by sequentially adding covariates to a baseline model (Figure 12). This approach involved three consecutive steps.

In the first step, we established a baseline model (Model 0) that included age, sex, and serum creatinine level, as the latter emerged as a significant predictor in the univariable analysis. In the second step, we individually added LVEF, LVGLS, or LVGCS to this baseline model, resulting in Models 1, 2, and 3, respectively. Among these, the model incorporating LVGLS (Model 2) demonstrated the lowest AIC value (Figure 12A). In the third step, we further refined the analysis by adding RVEF, RVGLS, or RVGCS to Model 2, yielding Models 4, 5, and 6, respectively. Of these, the model containing RVGCS (Model 6) exhibited the lowest AIC (Figure 12B). In this final model, age and RVGCS emerged as independent predictors of all-cause mortality, whereas sex, serum creatinine level, and LVGLS did not demonstrate independent prognostic significance (Table 12).

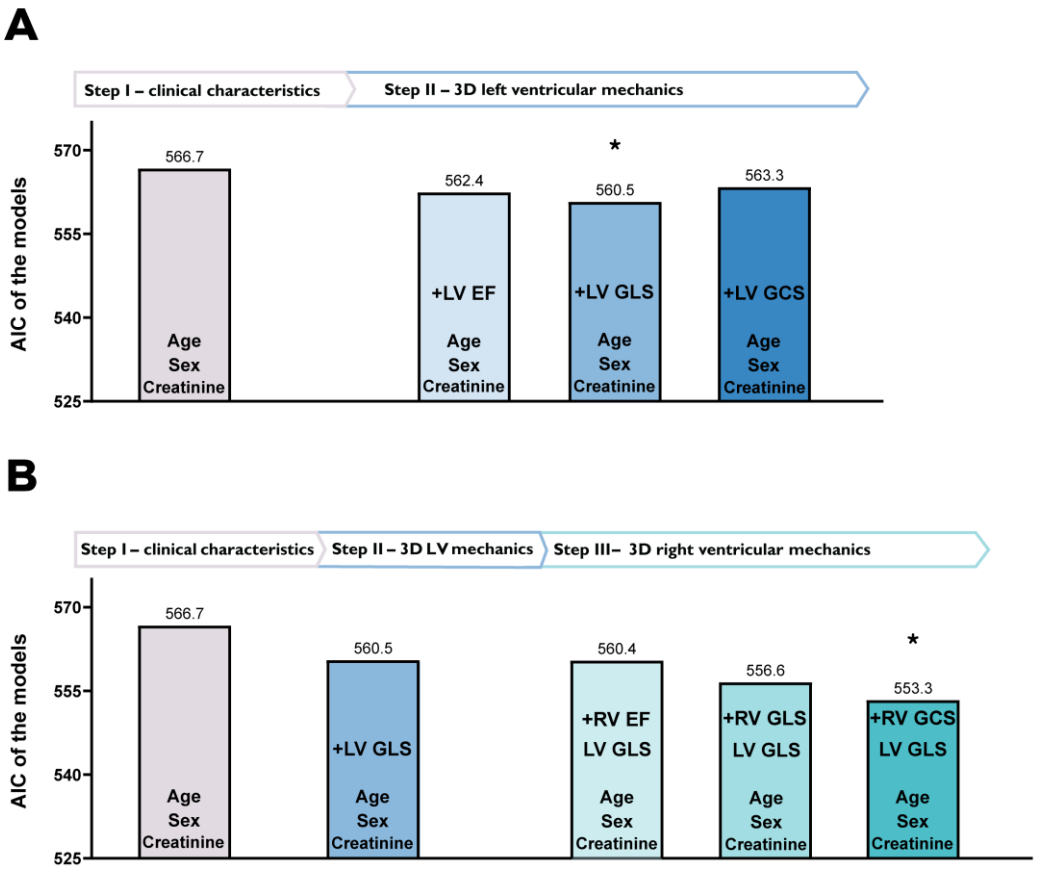

Figure 12. *Identification of the best-fit models, including LV and RV functional parameters by multivariable Cox regression analysis based on AIC. (A) Depicts different models with only clinical characteristics (Step I) and 3D LV mechanical parameters added one by one (Step II). In Step II, adding LVGLS to the model resulted in the lowest (best) AIC value. (B) Shows the added value of 3D RV mechanical parameters (Step III). In Step III, adding RVGCS to the previously established model in Step II (clinical characteristics and LVGLS) resulted in the best fit to our data, as confirmed by the lowest AIC value (44).*

Table 12. Independent predictors of all-cause mortality identified using multivariable Cox regression

	Multivariable Cox regression	
	HR [95% CI]	**p**
Age	1.036 [1.011 – 1.061]	**0.004**
Sex	0.690 [0.376 – 1.266]	0.231
Creatinine	1.005 [0.999 – 1.012]	0.087
LVGLS	1.017 [0.963 – 1.075]	0.543
RVGCS	1.091 [1.032 – 1.152]	**0.002**

CI: confidence interval, HR: hazard ratio, LVGLS: left ventricular global longitudinal strain, RVGCS: right ventricular global circumferential strain

We have confirmed that our approach identified the optimal combination of covariates by constructing multivariable models incorporating all possible combinations of LV and RV parameters (Table 13).

Table 13. Akaike information criterion values of multivariable Cox regression models

Step I	Step II	Step III	AIC
Age + sex + creatinine	+LVEF	+RVEF	561.4
		+RVGLS	556.8
		+RVGCS	553.6
	+LVGLS	+RVEF	560.4
		+RVGLS	556.6
		+RVGCS	***553.3***
	+LVGCS	+RVEF	561.5
		+RVGLS	556.8
		+RVGCS	553.6

EF: ejection fraction, GCS: global circumferential strain, GLS: global longitudinal strain, LV: left ventricle, RV: right ventricle

4.3.5. Comparison of the discriminatory power by receiver-operator characteristic analysis

On ROC analysis, LVGLS demonstrated the highest discriminative power among LV functional parameters (area under the ROC curve: 0.644 [95% CI: 0.561 – 0.726, p<0.001]). Nevertheless, RVGCS exhibited the highest discriminative power among all evaluated 2DE and 3DE parameters (0.690 [95% CI: 0.614 – 0.765, p<0.001] (44).

4.3.6. Subgroup analysis

As the model incorporating LVGLS and RVGCS was identified as the optimal model among those evaluated, we stratified patients into four subgroups based on the median values of LVGLS (−15.9%) and RVGCS (−17.9%). Group 1 comprised patients with both LVGLS and RVGCS above the median, whereas Group 4 included patients with both parameters below the median. Group 2 consisted of patients with LVGLS below the median and RVGCS above the median, while Group 3 included those with LVGLS above the median and RVGCS below the median (Figure 13).

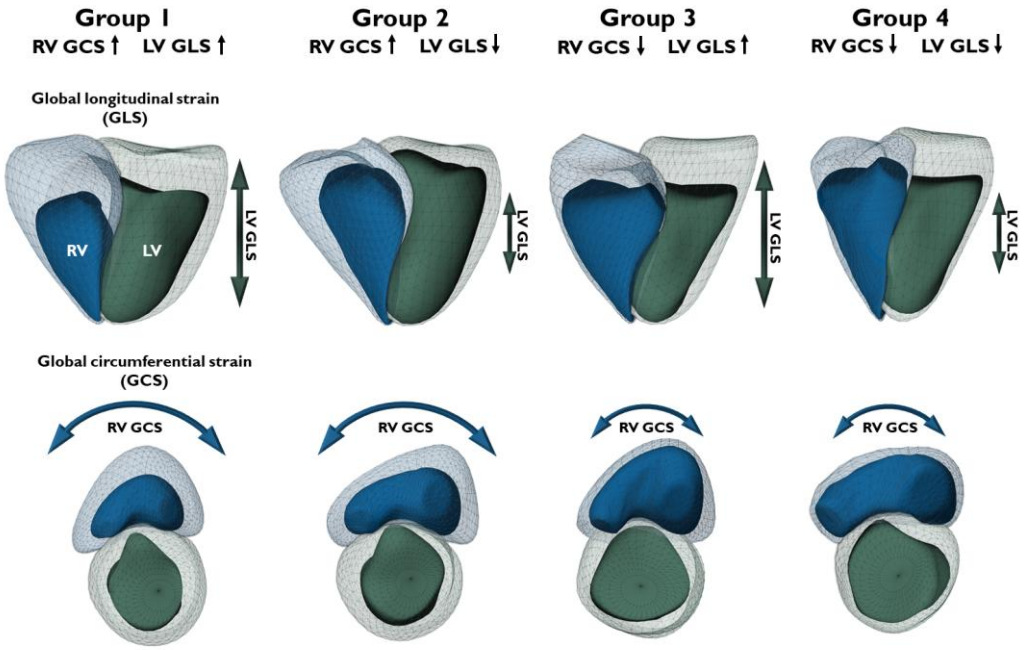

Figure 13. *3D schematic models depict representative cases of different biventricular mechanical patterns in patients from the respective groups. The four groups were divided based on the median values of LVGLS (−15.9%) and RVGCS (−17.9%). Upward arrows represent strain values better than the median (more negative), downward arrows represent strain values worse than the median (less negative). Light green mesh – LV EDV; dark green surface – LV ESV; light blue mesh – RV EDV; dark blue surface – RV ESV. Smaller double-headed arrows represent strain values worse than the median: green arrow – LVGLS; blue arrow – RVGCS (44).*

Among the 125 patients in Group 1, 37 (30%) were HTX recipients, 19 (15%) were evaluated prior to atrial fibrillation ablation, 18 (14%) had aortic stenosis, and 51 (41%) had mitral valve disease. Group 2 comprised 53 patients, including 16 (30%) with HFrEF, 11 (21%) HTX recipients, 6 (11%) evaluated before atrial fibrillation ablation, and 20 (38%) with aortic stenosis. Group 3 included 54 patients, of whom 1 (2%) had HFrEF, 30 (56%) were HTX recipients, 8 (15%) had aortic stenosis, and 15 (28%) had mitral valve disease. Group 4 consisted of 125 patients, including 78 (62%) with HFrEF, 13 (10%) HTX recipients, 33 (26%) with aortic stenosis, and 1 (1%) with mitral valve disease.

In Group 1, 7.2% of patients died during the follow-up period, whereas in Group 2, the mortality rate was 7.5%. In contrast, adverse outcomes were more frequent in Groups 3 and 4, with mortality rates of 20.3% and 24.8%, respectively. These differences in survival among the subgroups were illustrated using Kaplan-Meier curves (Figure 14).

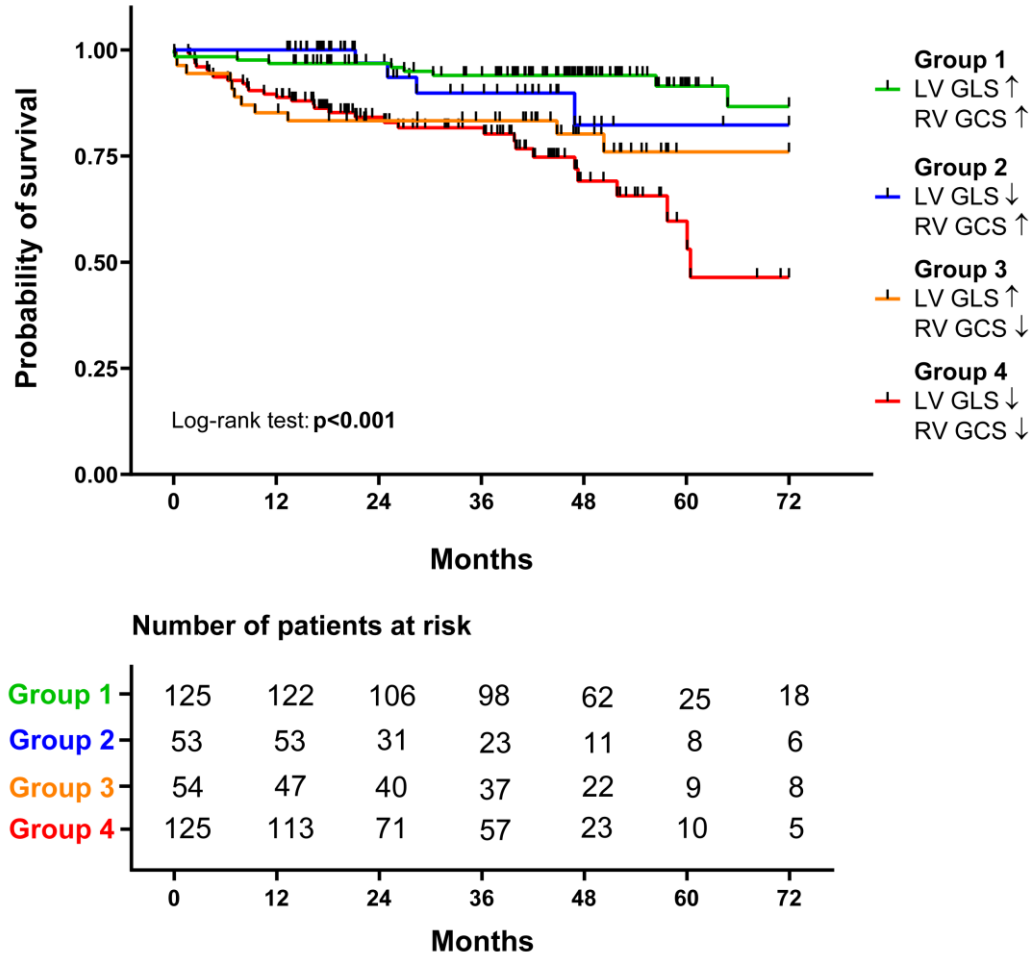

Figure 14. *Survival analysis of the different groups. Based on the respective median values of LVGLS (−15.9%) and RVGCS (−17.9%), patients were divided into four groups. The survival of the four groups is visualized on Kaplan-Meier curves, and the log-rank test was performed for comparison (44).*

Patients with both LVGLS and RVGCS below the median (Group 4) exhibited a more than fivefold increased risk of death compared with those in Group 1 and more than a threefold higher risk compared with Group 2. Interestingly, no significant difference in mortality was observed between Group 3 (with LVGLS above the median) and Group 4, but being categorized into Group 3 vs. Group 1 still held a more than 3-fold risk (Table 14).

Table 14. Hazard ratios of all-cause mortality in the different subgroups

Cox proportional-hazards models		
	HR [95% CI]	**p**
Group 2 vs. Group 1	1.489 [0.453 – 4.886]	0.512
Group 3 vs. Group 1	3.099 [1.284 – 7.484]	**0.012**
Group 4 vs. Group 1	5.089 [2.399 – 10.793]	**<0.001**
Group 3 vs. Group 2	2.351 [0.741 – 7.459]	0.147
Group 4 vs. Group 2	3.565 [1.256 – 10.122]	**0.017**
Group 4 vs. Group 3	1.515 [0.756 – 3.036]	0.241

CI: confidence interval, HR: hazard ratio

Regarding the baseline characteristics of these groups, patients in Group 4 were older, exhibited lower systolic blood pressure, and had a higher prevalence of diabetes, coronary artery disease, and prior ICD implantation (44). This group also demonstrated the highest serum creatinine levels among all subgroups. In contrast, Group 3 consisted of relatively younger patients, with lower frequencies of diabetes, coronary artery disease, and atrial fibrillation in their medical history. Group 4 patients also had the largest LV, RV, and RA dimensions, as well as the highest E/e′ values; however, LAVi and RVSP did not significantly differ across the four groups (44). The 3DE parameters of the subgroups are presented in Table 15. In addition to the pronounced chamber dilation and biventricular functional impairment observed in Group 4, patients in Group 3 exhibited the lowest LVMi while maintaining preserved mean LV and RVEF (60 ± 5% and 49 ± 6%, respectively).

Table 15. 3D echocardiographic parameters

	Group 1 (n=125)	Group 2 (n=53)	Group 3 (n=54)	Group 4 (n=125)	Overall p
Left ventricle					
LVEDVi (ml/m²)	74.7±24.9[d]	74.1±26.8[d]	66.9±21.4[d]	100.6±36.8[abc]	**<0.001**
LVESVi (ml/m²)	28.4±9.2[bd]	43.9±24.3[acd]	26.5±9.0[bd]	70.0±35.5[abc]	**<0.001**
LVSVi (ml/m²)	46.3±16.8[bcd]	30.3±8.1[ac]	40.4±13.5[abd]	30.6±8.2[ac]	**<0.001**
LVMi (g/m²)	84.4±25.3[bd]	109.2±39.0[acd]	82.5±24.1[bd]	127.9±34.8[abc]	**<0.001**
LVEF (%)	60.8±4.9[bd]	45.2±12.4[acd]	60.3±5.4[bd]	34.0±13.4[abc]	**<0.001**
LVGLS (%)	-20.5±3.2[bd]	-12.2±3.1[acd]	-19.4±3.4[bd]	-9.5±3.5[abc]	**<0.001**
LVGCS (%)	-30.3±3.8[bd]	-21.9±7.6[acd]	-30.6±4.1[bd]	-15.6±7.9[abc]	**<0.001**
Right ventricle					
RVEDVi (ml/m²)	65.2±16.8[d]	61.6±19.5[d]	65.0±17.8[d]	81.1±28.9[abc]	**<0.001**
RVESVi (ml/m²)	29.6±8.5[d]	30.3±12.4[d]	33.4±11.1[d]	50.2±23.8[abc]	**<0.001**
RVSVi (ml/m²)	35.6±9.4[bcd]	31.3±8.5[a]	31.6±8.1[a]	30.9±8.6[a]	**0.001**
RVEF (%)	54.7±4.4[bcd]	52.0±5.9[acd]	48.8±5.9[abd]	40.1±9.5[abc]	**<0.001**
RVGLS (%)	-20.3±3.9[bcd]	-16.2±3.2[ad]	-17.2±4.0[ad]	-12.3±3.9[abc]	**<0.001**
RVGCS (%)	-23.2±3.5[bcd]	-21.4±3.2[acd]	-14.2±3.6[abd]	-12.1±3.6[abc]	**<0.001**

Continuous variables are presented as means ± SD, categorical variables are reported as frequencies (%). a: p < 0.05 vs. Group 1, b: p < 0.05 vs. Group 2, c: p < 0.05 vs. Group 3, d: p < 0.05 vs. Group 4 EDVi: end-diastolic volume index, EF: ejection fraction, ESVi: end-systolic volume index, GCS: global circumferential strain, GLS: global longitudinal strain, LV: left ventricle, Mi: mass index, RV: right ventricle, Svi: stroke volume index

4.3.7. Reproducibility

Intraobserver and interobserver variability were assessed. The first reader repeated the analysis in a randomly selected subset of patients (n = 15), blinded to the initial results. The same subset was independently analyzed by a second reader, also in a blinded manner. ICC values for RVGCS were lower than those for RVEF and RVGLS; however, they remained within an acceptable range (Table 16).

Table 16. Intra- and interobserver variability of 3D right ventricular functional metrics

	Intraclass correlation coefficient [95% CI]	
	Intraobserver	**Interobserver**
RVEF	0.966 [0.902 – 0.988]	0.971 [0.918 – 0.990]
RVGLS	0.935 [0.823 – 0.978]	0.767 [0.437 – 0.915]
RVGCS	0.888 [0.700 – 0.961]	0.753 [0.416 – 0.909]

CI: confidence interval, EF: ejection fraction, GCS: global circumferential strain, GLS: global longitudinal strain, RV: right ventricle

5. Discussion

5.1. Investigating the added predictive value of right ventricular ejection fraction compared with conventional echocardiographic measurements in patients who underwent diverse cardiovascular procedures

In our first study, we examined a diverse cohort of patients with left-sided heart disease undergoing various cardiac interventional or surgical procedures, utilizing 3DE for RV functional assessment. Our findings indicated that conventional echocardiographic parameters may be insufficient for refined risk stratification in this population. In contrast, RVEF derived from 3DE emerged as a robust clinical predictor of adverse outcomes. We extended the existing knowledge by focusing on a high-risk cohort primarily composed of patients with HFrEF or severe valvular heart disease. Importantly, these patients were at elevated risk not only due to their baseline functional status, but also due to prior or impending invasive procedures and their associated complications (41, 45). A head-to-head comparison between RVEF and conventional RV function metrics demonstrated the superior prognostic value of RVEF in predicting 2-year all-cause mortality. The optimal cut-off values identified through ROC analysis were consistent with current guideline-based thresholds for RVEF, FAC, and FWLS. However, for TAPSE, the optimal threshold was 24 mm, which is well within the conventional "normal" range, given that RV dysfunction is defined by values below 17 mm (24). This finding suggests that TAPSE may be of limited utility in certain clinical scenarios and underscores the need for context-specific interpretation. We hypothesize that this unexpected result may be influenced by patients with severe MR, in whom increased longitudinal shortening, which was previously thought to be protective, may in fact represent maladaptive remodeling. In such cases, "supernormal" TAPSE may paradoxically reflect adverse functional changes associated with worse perioperative outcomes (41).

5.2. Evaluating the disagreement between conventional parameters and 3D echocardiography-derived ejection fraction in the detection of right ventricular systolic dysfunction and its association with outcomes

In the second study, we investigated the discordance between TAPSE, FAC, FWLS, and 3DE-derived RVEF in diagnosing RV systolic dysfunction in a large and diverse cohort of patients with various cardiac conditions. We found that RV dysfunction identified by conventional parameters, using guideline-recommended cut-off values, demonstrated only modest agreement with RVEF-based classification, underscoring the limited concordance between these methods. The degree of reclassification of RV systolic dysfunction was high, reaching 49% for FAC and 46% for TAPSE in the overall cohort. Importantly, reclassification of RV function based on RVEF was associated with significantly different clinical outcomes. The rate of reclassification varied according to the specific parameter and the underlying pathology, highlighting the influence of disease-specific RV contraction patterns on functional assessment (46, 47). Among the conventional parameters, FWLS exhibited the strongest agreement with RVEF-defined dysfunction, suggesting that it may offer a more comprehensive reflection of RV performance than TAPSE or FAC. These findings reinforce the limitations of relying on a single 2DE-based metric and support the use of a multiparametric approach by combining at least two conventional measures when 3DE is not available, to improve the accuracy and clinical relevance of RV functional assessment. Of note, patients with normal RVEF but abnormal TAPSE or FAC experienced worse outcomes than those with normal RVEF and also normal TAPSE or FAC, respectively. This phenomenon again highlights that subclinical changes in the RV contraction pattern might have added clinical value in the face of a maintained RVEF.

5.3. Assessing the prognostic significance of RV circumferential strain

In our third study, we sought to evaluate the prognostic significance of circumferential shortening in both the LV and RV using 3DE. We found that reduced LV and RVGCS were significantly associated with all-cause mortality in univariable Cox regression analyses. When tested in various multivariable models, the combination of LVGLS and RVGCS demonstrated the best model fit. Interestingly, only RVGCS emerged as an independent predictor of mortality, whereas LVGLS and serum creatinine levels did not

retain statistical significance. To further explore the prognostic implications, we stratified the population into four groups based on the median values of LVGLS and RVGCS. These groups showed clear differences in survival, and notably, patients with preserved LVGLS but impaired RVGCS experienced significantly worse outcomes. This finding underscores the incremental prognostic value of RV circumferential mechanics and suggests that RVGCS may capture critical aspects of ventricular performance that are not reflected by traditional LV and RV function measures.

5.4. Conventional and three-dimensional echocardiography-based assessment of right ventricular function

Compared to the relatively simple conical shape of the LV, the morphology and contraction pattern of the RV are considerably more complex. The biplane Simpson's method, performed by contouring the LV endocardial borders in both the apical four-chamber and apical two-chamber views, offers a straightforward and relatively accurate approach to LV volume quantification and is therefore widely used in clinical practice. However, no comparable 2DE-based method exists for the RV, as its intricate geometry and multidirectional mechanics limit the applicability of standard imaging techniques (11).

Thus, surrogate measures of RV systolic function are applied in the echocardiographic routine. Conventional echocardiographic parameters have long been utilized as reliable indicators of RV systolic function. These parameters, while widely used, provide only a limited representation of RV function, as their one- or two-dimensional nature fails to capture the RV's complex 3D geometry and contractile patterns, thereby reducing their accuracy in assessing systolic function and predicting adverse clinical outcomes, potentially limiting their ability to fully capture the spectrum of RV dysfunction and predict associated adverse clinical outcomes (11, 24). Consequently, their sensitivity and specificity in identifying subtle alterations in RV function are compromised, as our results suggest (43).

TAPSE, the S′ wave measured by TDI, and FWLS assessed by speckle-tracking echocardiography all reflect only the longitudinal shortening of the RV, typically derived

from a single apical four-chamber view. These parameters, while widely used, inherently neglect the other two essential axes of RV geometry and function: radial and anteroposterior contraction. Radial shortening, which is defined by the inward motion of the RV free wall, generates the so-called “bellows effect,” which significantly contributes to SV. Additionally, anteroposterior shortening, resulting from the traction exerted by the LV’s circumferential contraction on the RV free wall insertion points, also plays a critical role in RV ejection. By ignoring these multidirectional components, longitudinal parameters alone provide an incomplete representation of RV systolic performance (48).

Traditionally, RV longitudinal shortening has been regarded as the principal determinant of global RV function; consequently, there has been a prevailing clinical perception that TAPSE serves as a comprehensive measure of RV performance (49). However, recent investigations by our research group in healthy volunteers have demonstrated that radial and anteroposterior motion components are at least equally important contributors to overall RV ejection (47). While FAC partially reflects radial function, it is still derived from a single imaging plane and therefore offers only a limited representation of the RV’s complex 3D geometry. Notably, routine 2DE parameters entirely neglect anteroposterior motion, despite its functional significance (38, 50). Even relatively subtle inward movements in these radial and anteroposterior directions can generate substantial SV, due to the large surface area of the RV free wall (49).

These observations not only support the clinical utility of 3DE in RV assessment but also gain further relevance in the context of disease-specific alterations in contraction patterns. For instance, in conditions characterized by RV pressure overload, radial contraction of the RV free wall deteriorates early, whereas longitudinal shortening is often preserved until more advanced stages (51). As a result, TAPSE and other measures of RV longitudinal contraction may fail to detect early dysfunction and may overestimate global RV performance. Similarly, in patients undergoing cardiac surgery involving pericardiotomy, the loss of pericardial constraint leads to a reduction in longitudinal shortening that is typically offset by compensatory enhancement of radial motion, thereby preserving global RVEF (52, 53). In such cases, TAPSE may substantially underestimate RV function (41). Given that the mechanical contribution of different motion components

varies depending on the underlying pathology, the diagnostic reliability of conventional 2DE surrogates is inherently limited.

In recent years, the advent of 3DE has significantly enhanced our understanding of cardiac anatomy and function. The 3DE technique allows for accurate volumetric assessment of the RV, providing a more comprehensive evaluation of its contractile performance. Reference values of RV volumes and EF are available to differentiate normal from abnormal RV (54, 55). Moreover, since it takes into account both the longitudinal and the radial component of the endocardial motion and includes the RV outflow tract contribution, RVEF derived from the volumetric data offers a more comprehensive quantification of RV systolic function compared to traditional 2DE parameters and shows excellent agreement with RVEF obtained with CMR (56, 57).
In contrast to 2DE measures, RVEF derived from 3DE provides an integrated and robust measure of RV systolic performance that remains valid across a wide range of clinical scenarios. This broad applicability makes RVEF a compelling candidate for risk stratification and prognostic evaluation in unselected and heterogeneous patient populations. The independent prognostic value of 3DE-derived RVEF has been extensively demonstrated in various patient populations (39, 57-60). Nagata et al. were among the first to publish the prognostic significance of RVEF (57). In their study comprising 446 patients with diverse cardiovascular pathologies, subjects were followed up to cardiac death and major adverse cardiovascular events (MACE) (57). RVEF demonstrated a significant association with cardiac death and MACE, comparable to E/e' and LVEF, and retained its prognostic relevance for future cardiac events even after adjustment for relevant clinical and echocardiographic covariates. Later, Surkova et al. conducted a retrospective investigation involving a large cohort of patients with various cardiovascular diseases (39). Their findings demonstrated that reduced RVEF was independently associated with both all-cause mortality and cardiac death after adjustment for clinical and echocardiographic variables (39). Furthermore, RVEF exhibited superior sensitivity and specificity in predicting all-cause mortality compared to conventional RV systolic function parameters, such as TAPSE and FAC, and its impairment was associated with a significantly elevated mortality risk independent of LVEF. The authors further stratified patients into four groups based on preserved or reduced LVEF and/or RVEF.

Survival analysis revealed significant differences among these groups: patients with reduced RVEF and preserved LVEF exhibited higher rates of all-cause mortality and cardiac death than those with reduced LVEF and preserved RVEF, and their outcomes were comparable to those with biventricular dysfunction (39). These two research groups also established RVEF cut-off values (45%, 40%, and 30%) that stratify patient cohorts according to risk, and consequently recommended their incorporation into routine clinical practice (61). A recent meta-analysis has verified that RV dysfunction is strongly associated with all-cause mortality and adverse cardiopulmonary outcomes in patients with diverse cardiopulmonary diseases, further highlighting its superior prognostic value compared to conventional echocardiographic parameters of RV function (62). Specifically, a 1 SD reduction in 3DE-derived RVEF exhibited a significantly stronger association with adverse events than an equivalent change in TAPSE, FAC, or FWLS (62).

Nevertheless, the 3DE-based evaluation of RV size and systolic function has not been widely adopted in routine clinical practice (63-65). Despite the above-mentioned advantages, 3DE remains subject to important limitations. High-quality image acquisition requires optimal acoustic windows and operator expertise, which can be challenging in patients with poor echocardiographic windows, arrhythmias, or tachycardia, conditions that may distort image stitching or degrade temporal resolution. Additionally, RV endocardial border delineation can be difficult in cases of trabeculated or dilated ventricles, potentially affecting volume accuracy (24, 66). Moreover, while semi-automated analysis tools have improved efficiency, manual adjustments are still often necessary, introducing some degree of operator dependency. As 3D technology and post-processing algorithms continue to evolve, these limitations are progressively being addressed, reinforcing the role of 3DE as a powerful tool in the comprehensive assessment of RV function across a range of cardiovascular diseases.

Many experts recommend a multiparametric approach combining qualitative assessments with various conventional quantitative metrics of RV systolic function in centers without established experience in 3DE-based evaluation of RV size and function (65). However, there remains no standardized framework for integrating these diverse RV parameters

into a comprehensive assessment of RV function or for guiding clinical decision-making. Our findings show that RV systolic dysfunction identified by two or more conventional echocardiographic parameters is associated with a significantly worse prognosis compared to cases with only a single abnormal parameter (43). This strategy may aid in risk stratification when 3DE assessment is not available or feasible. Additionally, we identified patient subgroups with the highest rates of RV function reclassification based on specific conventional parameters, thereby supporting the selection of the most appropriate metric(s) according to the underlying cardiac pathology and in line with precision medicine principles.

5.5. Right ventricular longitudinal and non-longitudinal mechanics and their prognostic value

Recent advances in echocardiographic hardware and software have enabled the automated, accurate quantification of myocardial mechanics. Notably, GLS assessed by 2D speckle tracking echocardiography has become a cornerstone parameter for evaluating LV systolic function. Reflecting the behavior of subendocardial longitudinal fibers, LVGLS is more sensitive to subtle dysfunction than conventional measures such as LVEF. A meta-analysis of 16 studies demonstrated the superior prognostic value of LVGLS over LVEF for predicting major adverse cardiac events across various cardiac conditions. GLS is now a well-validated and reproducible metric for assessing LV longitudinal deformation, and its integration into routine clinical practice is expected in the near future (67).

Nevertheless, in addition to longitudinal shortening, circumferential shortening contributes substantially to global systolic function in both ventricles. A mathematical model demonstrated that LVGCS has more than twice the impact on LVEF compared to LVGLS, and even a modest increase in LVGCS can offset a significant reduction in LVGLS (68). LVEF is quadratically related to circumferential shortening but only linearly dependent on longitudinal shortening (49). Although LVGCS has been reported using 2DE, its calculation is complex (requiring analysis of three parasternal short-axis levels) and suffers from poor reproducibility, leading most software vendors to discontinue its measurement (69, 70). By contrast, 3DE enables the assessment of both

LVGCS and LVGLS from a single acquisition within the same cardiac cycle, potentially overcoming the limitations of 2DE-based methods.

Importantly, circumferential shortening contributes significantly to global RV pump function and can be assessed exclusively using 3DE (49). Notably, even subtle impairments in the circumferential shortening of the extensive RV free wall may lead to significant global functional deterioration (71). Circumferential shortening results from the inward motion of the RV free wall (radial shortening) and the traction of the free wall insertion points toward each other, mediated by LV contraction (anteroposterior shortening) (37). Beyond this mechanical linkage, accumulating evidence indicates that LV-RV interactions occur on multiple levels: changes in geometry, loading conditions, or contractility of one ventricle profoundly affect the other (72). This intricate interplay underscores that nearly every pathological process may impact both sides of the interventricular septum, carrying diagnostic and prognostic implications.

With the increasing appreciation of LV-RV interactions, detailed evaluation of the RV has gained substantial attention. Similar to the LV, assessment of RV deformation may offer greater diagnostic and prognostic value than RVEF alone. Although small cohort studies in various RV pathologies, such as pulmonary hypertension, atrial septal defect, and post-cardiac surgery, have identified specific alterations in RV mechanics, these studies have primarily employed simple 2DE-derived functional parameters. (73-75).

The ReVISION method enables the quantification of the relative contributions of longitudinal, radial, and anteroposterior motion components to global RV function, as well as the assessment of 3D RVGLS and RVGCS, based on 3DE-derived models (38). In a study involving 300 healthy volunteers, Lakatos et al. demonstrated that circumferential EF, indexed to global RVEF, was clearly predominant compared with longitudinal EF. Contrary to the traditional perspective, they found that the relative contributions of radial and anteroposterior motion are comparable to those of longitudinal shortening in determining global RV function. These findings suggest that conventional parameters focused solely on longitudinal shortening may be insufficient for a comprehensive characterization of RV function (47).

Using the same approach, two studies have already demonstrated the added prognostic value of RV non-longitudinal functional parameters. Kitano et al. investigated a relatively large cohort of patients with various cardiac diseases, showing that RV 3D strain parameters were significantly associated with hard clinical endpoints, even after adjustment for multiple clinical covariates (76). Similarly, Surkova et al. studied consecutive patients with left-sided heart disease and found that, even among those with preserved LVEF, the anteroposterior component of total RVEF emerged as a significant and independent predictor of outcomes (46). Our findings further strengthen the evidence supporting the diagnostic and prognostic importance of RV non-longitudinal shortening (44). As a previously neglected marker of ventricular systolic performance, circumferential deformation may capture a novel dimension of RV function with established prognostic relevance (49). RVGCS, in particular, may serve as a robust and universal biomarker reflecting the overall cardiopulmonary status, outperforming conventional echocardiographic measures and correlating with adverse clinical outcomes not only in classical right heart diseases but also in primary left heart conditions (49). Nevertheless, the precise pathophysiological mechanisms underlying circumferential shortening impairment, such as ventricular interdependence and RV pressure overload, and the potential utility of RVGCS as a screening tool warrant further investigation.

Two recent publications contribute to the knowledge on novel strain metrics and underscore their importance in different clinical scenarios. In particular, Ladányi et al. employed these parameters to investigate the mechanical adaptation of the RV in the context of secondary tricuspid regurgitation and its association with clinical outcomes. Their study demonstrated that patients with ventricular etiology of secondary tricuspid regurgitation exhibited significantly lower absolute values of RVGCS compared to those with atrial etiology (77). In another study, implementing intraoperative transesophageal 3DE during cardiac surgery, Keller et al. found significant reductions in RV GLS and GCS in patients experiencing adverse postoperative outcomes. Although LVEF was also reduced in these patients, it did not differ significantly between the outcome groups. In contrast, RV strain parameters demonstrated significant differences between the groups, underscoring their potential prognostic value in this clinical setting (78).

5.6. Limitations

Several limitations have to be acknowledged regarding the above-discussed studies. First, an inherent limitation of our studies is their single- or two-center retrospective design and the application of specific inclusion criteria (i.e., the availability of good-quality 3DE recordings) that may have introduced selection bias. Second, HTX recipients represent a distinct cohort within our studies, characterized by unique clinical and hemodynamic profiles that differ substantially from those observed in conventional left-heart disease populations. To address this potential source of heterogeneity, we performed additional analyses in our third study to confirm that their inclusion did not introduce bias regarding these findings (44). Third, in some cases, low event numbers limited the construction of multivariable models. Fourth, although 3DE-derived RVEF is not considered the gold standard, it should be noted that no true gold standard parameter of RV function exists, aside from invasively obtained pressure–volume loop measurements, which are not feasible in large population studies (79). Ideally, contractility, defined as the myocardium's intrinsic capacity to shorten independently of loading conditions, would serve as the primary metric of functional assessment; however, conventional parameters, including RVEF, predominantly reflect ventriculo-arterial coupling rather than pure contractility (80). The 3DE software platforms employed in our studies are clinically well validated and have demonstrated good agreement with RVEF measurements derived from CMR imaging (56, 57). Fifth, the −20% cut-off for FWLS recommended in current guidelines was established using data obtained from a software platform different from that employed in our studies (24). Nevertheless, analysis of previously published data from healthy individuals assessed with TomTec's 4D RV-Function 2 software indicates that the −20% threshold remains applicable and valid (47). Sixth, due to the lack of cause-specific mortality data, we could not investigate the association between the RV systolic functional parameters and cardiac death. Seventh, due to the retrospective design, neither sample size calculation nor post hoc power analysis was performed, which may limit the interpretability of subgroup analyses. Lastly, the validity and generalizability of our results should be tested in prospective outcome studies in different races and clinical scenarios. Additionally, inter-vendor and inter-software reproducibility of the investigated parameters should be addressed in future prospective test–retest studies.

6. Conclusions

In our first study, we examined a heterogeneous cohort of patients receiving tertiary cardiology care and undergoing various cardiac procedures. We demonstrated that RVEF measured by 3DE is significantly associated with 2-year all-cause mortality and outperforms conventional RV functional parameters in predicting adverse outcomes. These findings support the routine clinical implementation of 3DE, as it offers valuable incremental information for both diagnostic and prognostic purposes. Nevertheless, larger-scale studies in more specific patient populations are needed to further delineate the utility of RVEF measurement in predicting diverse clinical endpoints and long-term outcomes.

In our second study, we found that guideline-recommended cut-off values for conventional echocardiographic parameters of RV systolic function exhibited only a modest association with RVEF as assessed by 3DE, and the extent of RV function reclassification varied according to the specific parameter employed and the underlying pathology. Among these, impaired FWLS demonstrated the strongest concordance with the RVEF cut-off. When 3DE evaluation is not feasible, a multiparametric approach to RV systolic function assessment is preferable. Notably, the presence of two or more conventional parameters indicating RV systolic dysfunction was associated with the poorest clinical outcomes.

Regarding our third study, RV circumferential shortening was shown to possess significant prognostic value for adverse clinical outcomes. RVGCS emerged as a robust and independent predictor of all-cause mortality in patients with left-sided cardiac disease. These findings underscore the clinical relevance of 3DE-derived myocardial mechanics parameters.

7. Summary

The RV, historically regarded as the "forgotten chamber," has gained increasing recognition for its crucial prognostic role in various cardiovascular pathologies. This doctoral thesis comprehensively evaluates RV systolic function using advanced echocardiographic modalities, emphasizing 3DE and strain-based techniques. The work is structured around three major studies that collectively interrogate the limitations of conventional RV function metrics, establish the prognostic value of 3DE-derived RVEF, and explore the incremental utility of RV deformation parameters, particularly RVGCS. In the first study, a heterogeneous cohort of patients undergoing diverse cardiovascular interventions was assessed to determine whether 3DE-derived RVEF offers incremental prognostic information beyond traditional echocardiographic indices. The findings demonstrated that RVEF was independently associated with two-year all-cause mortality and exhibited superior discriminatory power compared to parameters such as TAPSE, FAC, and FWLS, underscoring the value of volumetric RV assessment in refined risk stratification. The second study focused on the discordance between conventional RV function parameters and 3DE-derived RVEF in a large two-center population. A significant degree of reclassification was observed when RVEF served as the reference standard, with notable differences across distinct cardiac pathologies. Importantly, reclassification based on RVEF was strongly associated with divergent clinical outcomes, highlighting the limitations of isolated conventional parameters and advocating for a multiparametric approach where 3DE is unavailable. The third study assessed the prognostic implications of RV strain mechanics in patients with left-sided cardiac disease. Using 3DE-derived GLS and GCS, the study demonstrated that RVGCS emerged as an independent predictor of all-cause mortality, outperforming even LVGLS in multivariable models. Stratification based on combined LV and RV strain parameters revealed that patients with impaired RVGCS, regardless of LV strain status, faced markedly worse survival rates. Collectively, this thesis emphasizes the inadequacy of relying solely on traditional echocardiographic measures of RV function and substantiates the pivotal role of 3DE-derived metrics, especially RVEF and RVGCS, in contemporary cardiac risk assessment. These findings advocate for the integration of advanced RV functional parameters into routine clinical practice to enable more precise prognostication and personalized therapeutic strategies.

8. References

1. Rigolin VH, Robiolio PA, Wilson JS, Harrison JK, Bashore TM. The forgotten chamber: the importance of the right ventricle. Cathet Cardiovasc Diagn. 1995;35(1):18–28.

2. Haddad F, Hunt SA, Rosenthal DN, Murphy DJ. Right ventricular function in cardiovascular disease, part I: Anatomy, physiology, aging, and functional assessment of the right ventricle. Circulation. 2008;117(11):1436–1448.

3. Naeije R, Manes A. The right ventricle in pulmonary arterial hypertension. Eur Respir Rev. 2014;23(134):476–487.

4. Kaul S, Tei C, Hopkins JM, Shah PM. Assessment of right ventricular function using two-dimensional echocardiography. Am Heart J. 1984;107(3):526–531.

5. Hines R. Right ventricular function and failure: a review. Yale J Biol Med. 1991;64(4):295–307.

6. Santamore WP, Dell'Italia LJ. Ventricular interdependence: significant left ventricular contributions to right ventricular systolic function. Prog Cardiovasc Dis. 1998;40(4):289–308.

7. Oldershaw P. Assessment of right ventricular function and its role in clinical practice. Br Heart J. 1992;68(1):12–15.

8. Konstam MA, Kiernan MS, Bernstein D, Bozkurt B, Jacob M, Kapur NK, Kociol RD, Lewis EF, Mehra MR, Pagani FD, Raval AN, Ward C. Evaluation and Management of Right-Sided Heart Failure: A Scientific Statement From the American Heart Association. Circulation. 2018;137(20):e578–e622.

9. Ren X, Johns RA, Gao WD. EXPRESS: Right Heart in Pulmonary Hypertension: From Adaptation to Failure. Pulm Circ. 2019;9(3):2045894019845611.

10. Amsallem M, Mercier O, Kobayashi Y, Moneghetti K, Haddad F. Forgotten No More. JACC Heart Fail. 2018;6(11):891–903.

11. Rudski LG, Lai WW, Afilalo J, Hua L, Handschumacher MD, Chandrasekaran K, Solomon SD, Louie EK, Schiller NB. Guidelines for the echocardiographic assessment of the right heart in adults: a report from the American Society of Echocardiography endorsed by the European Association of Echocardiography, a registered branch of the European Society of Cardiology, and the Canadian Society of Echocardiography. J Am Soc Echocardiogr. 2010;23(7):685–713; quiz 786–688.

12. Bernal-Ramirez J, Díaz-Vesga MC, Talamilla M, Méndez A, Quiroga C, Garza-Cervantes JA, Lázaro-Alfaro A, Jerjes-Sanchez C, Henríquez M, García-Rivas G, Pedrozo Z. Exploring Functional Differences between the Right and Left Ventricles to Better Understand Right Ventricular Dysfunction. Oxid Med Cell Longev. 2021;2021:9993060.

13. Sheehan F, Redington A. The right ventricle: anatomy, physiology and clinical imaging. Heart. 2008;94(11):1510–1515.

14. Sanz J, Sánchez-Quintana D, Bossone E, Bogaard Harm J, Naeije R. Anatomy, Function, and Dysfunction of the Right Ventricle. JACC. 2019;73(12):1463–1482.

15. Vonk Noordegraaf A, Westerhof Berend E, Westerhof N. The Relationship Between the Right Ventricle and its Load in Pulmonary Hypertension. JACC. 2017;69(2):236–243.

16. Davlouros PA, Niwa K, Webb G, Gatzoulis MA. The right ventricle in congenital heart disease. Heart. 2006;92(suppl 1):i27–i38.

17. Berglund F, Piña P, Herrera CJ. Right ventricle in heart failure with preserved ejection fraction. Heart. 2020;106(23):1798–1804.

18. Melenovsky V, Hwang S-J, Lin G, Redfield MM, Borlaug BA. Right heart dysfunction in heart failure with preserved ejection fraction. Eur Heart J. 2014;35(48):3452–3462.

19. Bosch L, Lam CSP, Gong L, Chan SP, Sim D, Yeo D, Jaufeerally F, Leong KTG, Ong HY, Ng TP, Richards AM, Arslan F, Ling LH. Right ventricular dysfunction in left-sided heart failure with preserved versus reduced ejection fraction. Eur J Heart Fail. 2017;19(12):1664–1671.

20. Naeije R, Badagliacca R. The overloaded right heart and ventricular interdependence. Cardiovasc Res. 2017;113(12):1474–1485.

21. Friedberg MK, Redington AN. Right Versus Left Ventricular Failure. Circulation. 2014;129(9):1033–1044.

22. Schwarz K, Singh S, Dawson D, Frenneaux MP. Right Ventricular Function in Left Ventricular Disease: Pathophysiology and Implications. Heart Lung Circ. 2013;22(7):507–511.

23. Meyer P, Filippatos GS, Ahmed MI, Iskandrian AE, Bittner V, Perry GJ, White M, Aban IB, Mujib M, Dell'Italia LJ, Ahmed A. Effects of Right Ventricular Ejection

Fraction on Outcomes in Chronic Systolic Heart Failure. Circulation. 2010;121(2):252–258.

24. Lang RM, Badano LP, Mor-Avi V, Afilalo J, Armstrong A, Ernande L, Flachskampf FA, Foster E, Goldstein SA, Kuznetsova T, Lancellotti P, Muraru D, Picard MH, Rietzschel ER, Rudski L, Spencer KT, Tsang W, Voigt JU. Recommendations for cardiac chamber quantification by echocardiography in adults: an update from the American Society of Echocardiography and the European Association of Cardiovascular Imaging. J Am Soc Echocardiogr. 2015;28(1):1–39.e14.

25. Aloia E, Cameli M, D'Ascenzi F, Sciaccaluga C, Mondillo S. TAPSE: An old but useful tool in different diseases. Int J Cardiol. 2016;225:177–183.

26. Zaidi A, Knight DS, Augustine DX, Harkness A, Oxborough D, Pearce K, Ring L, Robinson S, Stout M, Willis J, Sharma V. Echocardiographic assessment of the right heart in adults: a practical guideline from the British Society of Echocardiography. Echo Res Pract. 2020;7(1):G19–G41.

27. Fredriksson AG, Zajac J, Eriksson J, Dyverfeldt P, Bolger AF, Ebbers T, Carlhäll C-J. 4-D blood flow in the human right ventricle. Am J Physiol Heart Circ Physiol. 2011;301(6):H2344–H2350.

28. Kadappu KK, Thomas L. Tissue Doppler Imaging in Echocardiography: Value and Limitations. Heart Lung Circ. 2015;24(3):224–233.

29. Muraru D, Haugaa K, Donal E, Stankovic I, Voigt JU, Petersen SE, Popescu BA, Marwick T. Right ventricular longitudinal strain in the clinical routine: a state-of-the-art review. Eur Heart J Cardiovasc Imaging. 2022;23(7):898–912.

30. Badano LP, Kolias TJ, Muraru D, Abraham TP, Aurigemma G, Edvardsen T, D'Hooge J, Donal E, Fraser AG, Marwick T, Mertens L, Popescu BA, Sengupta PP, Lancellotti P, Thomas JD, Voigt J-U, representatives I, Committee RTdwrbmotESD. Standardization of left atrial, right ventricular, and right atrial deformation imaging using two-dimensional speckle tracking echocardiography: a consensus document of the EACVI/ASE/Industry Task Force to standardize deformation imaging. Eur Heart J Cardiovasc Imaging. 2018;19(6):591–600.

31. Landzaat JWD, van Heerebeek L, Jonkman NH, van der Bijl EM, Riezebos RK. The quest for determination of standard reference values of right ventricular longitudinal systolic strain: a systematic review and meta-analysis. J Echocardiogr. 2023;21(1):1–15.

32. Kossaify A. Echocardiographic Assessment of the Right Ventricle, from the Conventional Approach to Speckle Tracking and Three-Dimensional Imaging, and Insights into the "Right Way" to Explore the Forgotten Chamber. Clin Med Insights Cardiol. 2015;9:65–75.

33. Wu VC, Takeuchi M. Echocardiographic assessment of right ventricular systolic function. Cardiovasc Diagn Ther. 2018;8(1):70–79.

34. Sugeng L, Mor-Avi V, Weinert L, Niel J, Ebner C, Steringer-Mascherbauer R, Bartolles R, Baumann R, Schummers G, Lang RM, Nesser HJ. Multimodality comparison of quantitative volumetric analysis of the right ventricle. JACC Cardiovasc Imaging. 2010;3(1):10–18.

35. Shimada YJ, Shiota M, Siegel RJ, Shiota T. Accuracy of Right Ventricular Volumes and Function Determined by Three-Dimensional Echocardiography in Comparison with Magnetic Resonance Imaging: A Meta-Analysis Study. J Am Soc Echocardiogr. 2010;23(9):943–953.

36. Lang RM, Badano LP, Tsang W, Adams DH, Agricola E, Buck T, Faletra FF, Franke A, Hung J, de Isla LP, Kamp O, Kasprzak JD, Lancellotti P, Marwick TH, McCulloch ML, Monaghan MJ, Nihoyannopoulos P, Pandian NG, Pellikka PA, Pepi M, Roberson DA, Shernan SK, Shirali GS, Sugeng L, Ten Cate FJ, Vannan MA, Zamorano JL, Zoghbi WA. EAE/ASE recommendations for image acquisition and display using three-dimensional echocardiography. J Am Soc Echocardiogr. 2012;25(1):3–46.

37. Lakatos B, Tősér Z, Tokodi M, Doronina A, Kosztin A, Muraru D, Badano LP, Kovács A, Merkely B. Quantification of the relative contribution of the different right ventricular wall motion components to right ventricular ejection fraction: the ReVISION method. Cardiovasc Ultrasound. 2017;15(1):8.

38. Tokodi M, Staub L, Budai A, Lakatos B, Csakvari M, Suhai F. Partitioning the right ventricle into 15 segments and decomposing its motion using 3D echocardiography-based models: the updated ReVISION method. Front Cardiovasc Med. 2021;8:622118.

39. Surkova E, Muraru D, Genovese D, Aruta P, Palermo C, Badano L. Relative prognostic importance of left and right ventricular ejection fraction in patients with cardiac diseases. J Am Soc Echocardiogr. 2019;32:1407–1415 e1403.

40. Magyar B, Tokodi M, Soós A, Tolvaj M, Lakatos BK, Fábián A, Surkova E, Merkely B, Kovács A, Horváth A. RVENet: A Large Echocardiographic Dataset

for the Deep Learning-Based Assessment of Right Ventricular Function. In: Karlinsky, L, Michaeli, T, Nishino, K (eds) Computer Vision - ECCV 2022 Workshops ECCV 2022 Lecture Notes in Computer Science. 2023;vol 13803.:569–583.

41. Tokodi M, Nemeth E, Lakatos B, Kispal E, Toser Z, Staub L. Right ventricular mechanical pattern in patients undergoing mitral valve surgery: a predictor of post-operative dysfunction? ESC Heart Fail. 2020;7:1246–1256.

42. Tolvaj M, Tokodi M, Lakatos BK, Fábián A, Ujvári A, Bakija FZ, Ladányi Z, Tarcza Z, Merkely B, Kovács A. Added predictive value of right ventricular ejection fraction compared with conventional echocardiographic measurements in patients who underwent diverse cardiovascular procedures. Imaging. 2021;13(2):130–137.

43. Tolvaj M, Kovács A, Radu N, Cascella A, Muraru D, Lakatos B, Fábián A, Tokodi M, Tomaselli M, Gavazzoni M, Perelli F, Merkely B, Badano LP, Surkova E. Significant Disagreement Between Conventional Parameters and 3D Echocardiography-Derived Ejection Fraction in the Detection of Right Ventricular Systolic Dysfunction and Its Association With Outcomes. J Am Soc Echocardiogr. 2024;37(7):677–686.

44. Tolvaj M, Fábián A, Tokodi M, Lakatos B, Assabiny A, Ladányi Z, Shiida K, Ferencz A, Schwertner W, Veres B, Kosztin A, Szijártó Á, Sax B, Merkely B, Kovács A. There is more than just longitudinal strain: Prognostic significance of biventricular circumferential mechanics. Front Cardiovasc Med. 2023;Volume 10 - 2023:1082725.

45. Tokodi M, Behon A, Merkel E, Kovacs A, Toser Z, Sarkany A. Sex-specific patterns of mortality predictors among patients undergoing cardiac resynchronization therapy: a machine learning approach. Front Cardiovasc Med. 2021;8:611055.

46. Surkova E, Kovács A, Tokodi M, Lakatos BK, Merkely B, Muraru D, Ruocco A, Parati G, Badano LP. Contraction Patterns of the Right Ventricle Associated with Different Degrees of Left Ventricular Systolic Dysfunction. Circ Cardiovasc Imaging. 2021;14(10):e012774.

47. Lakatos BK, Nabeshima Y, Tokodi M, Nagata Y, Toser Z, Otani K, Kitano T, Fabian A, Ujvari A, Boros AM, Merkely B, Kovacs A, Takeuchi M. Importance of Nonlongitudinal Motion Components in Right Ventricular Function: Three-Dimensional Echocardiographic Study in Healthy Volunteers. J Am Soc Echocardiogr. 2020;33(8):995–1005 e1001.

48. Kovacs A, Lakatos B, Tokodi M, Merkely B. Right ventricular mechanical pattern in health and disease: beyond longitudinal shortening. Heart Fail Rev. 2019;24:511–520.
49. Kovács A. Clinical Perspectives of Right Ventricular Function as Assessed by Three-Dimensional Echocardiography: Semmelweis University; 2024.
50. Surkova E, Kovács A, Lakatos B, Li W. Anteroposterior contraction of the systemic right ventricle: underrecognized component of the global systolic function. JACC Case Rep. 2021;3(5):728–730.
51. Bidviene J, Muraru D, Maffessanti F, Ereminiene E, Kovacs A, Lakatos B. Regional shape, global function and mechanics in right ventricular volume and pressure overload conditions: a three-dimensional echocardiography study. Int J Cardiovasc Imaging. 2021;37:1289–1299.
52. Lakatos B, Tokodi M, Assabiny A, Toser Z, Kosztin A, Doronina A. Dominance of free wall radial motion in global right ventricular function of heart transplant recipients. Clin Transplant. 2018;32:e13192.
53. Kovacs A, Lakatos B, Nemeth E, Merkely B. Response to Ivey-Miranda and Farrero-Torres “Is there dominance of free wall radial motion in global right ventricular function in heart transplant recipients or in all heart surgery patients?”. Clin Transplant. 2018;32:e13286.
54. Addetia K, Miyoshi T, Amuthan V, Citro R, Daimon M, Gutierrez Fajardo P, Kasliwal RR, Kirkpatrick JN, Monaghan MJ, Muraru D, Ogunyankin KO, Park SW, Ronderos RE, Sadeghpour A, Scalia GM, Takeuchi M, Tsang W, Tucay ES, Tude Rodrigues AC, Zhang Y, Hitschrich N, Blankenhagen M, Degel M, Schreckenberg M, Mor-Avi V, Asch FM, Lang RM. Normal Values of Left Ventricular Size and Function on Three-Dimensional Echocardiography: Results of the World Alliance Societies of Echocardiography Study. J Am Soc Echocardiogr. 2022;35(5):449–459.
55. Maffessanti F, Muraru D, Esposito R, Gripari P, Ermacora D, Santoro C, Tamborini G, Galderisi M, Pepi M, Badano LP. Age-, body size-, and sex-specific reference values for right ventricular volumes and ejection fraction by three-dimensional echocardiography: a multicenter echocardiographic study in 507 healthy volunteers. Circ Cardiovasc Imaging. 2013;6(5):700–710.
56. Muraru D, Spadotto V, Cecchetto A, Romeo G, Aruta P, Ermacora D, Jenei C, Cucchini U, Iliceto S, Badano LP. New speckle-tracking algorithm for right ventricular

volume analysis from three-dimensional echocardiographic data sets: validation with cardiac magnetic resonance and comparison with the previous analysis tool. Eur Heart J Cardiovasc Imaging. 2016;17(11):1279–1289.

57. Nagata Y, Wu VC-C, Kado Y, Otani K, Lin F-C, Otsuji Y, Negishi K, Takeuchi M. Prognostic Value of Right Ventricular Ejection Fraction Assessed by Transthoracic 3D Echocardiography. Circulation: Cardiovascular Imaging. 2017;10(2):e005384.

58. Nochioka K, Querejeta Roca G, Claggett B, Biering-Sørensen T, Matsushita K, Hung C-L, Solomon SD, Kitzman D, Shah AM. Right Ventricular Function, Right Ventricular–Pulmonary Artery Coupling, and Heart Failure Risk in 4 US Communities: The Atherosclerosis Risk in Communities (ARIC) Study. JAMA Cardiol. 2018;3(10):939–948.

59. Vîjîiac A, Onciul S, Guzu C, Verinceanu V, Bătăilă V, Deaconu S, Scărlătescu A, Zamfir D, Petre I, Onuţ R, Scafa-Udriste A, Vătășescu R, Dorobanţu M. The prognostic value of right ventricular longitudinal strain and 3D ejection fraction in patients with dilated cardiomyopathy. Int J Cardiovasc Imaging. 2021;37(11):3233–3244.

60. Meng Y, Zhu S, Xie Y, Zhang Y, Qian M, Gao L, Li M, Lin Y, Wu W, Wang J, Yang Y, Lv Q, Zhang L, Li Y, Xie M. Prognostic Value of Right Ventricular 3D Speckle-Tracking Strain and Ejection Fraction in Patients With HFpEF. Front Cardiovasc Med. 2021;8:694365.

61. Muraru D, Badano L, Nagata Y, Surkova E, Nabeshima Y, Genovese D. Development and prognostic validation of partition values to grade right ventricular dysfunction severity using 3D echocardiography. Eur Heart J Cardiovasc Imaging. 2020;21:10–21.

62. Sayour AA, Tokodi M, Celeng C, Takx RAP, Fábián A, Lakatos BK, Friebel R, Surkova E, Merkely B, Kovács A. Association of Right Ventricular Functional Parameters With Adverse Cardiopulmonary Outcomes: A Meta-analysis. J Am Soc Echocardiogr. 2023;36(6):624–633.e628.

63. Ajmone Marsan N, Michalski B, Cameli M, Podlesnikar T, Manka R, Sitges M, Dweck MR, Haugaa KH. EACVI survey on standardization of cardiac chambers quantification by transthoracic echocardiography. Eur Heart J Cardiovasc Imaging. 2020;21(2):119–123.

64. Schneider M, Aschauer S, Mascherbauer J, Ran H, Binder C, Lang I, Goliasch G, Binder T. Echocardiographic assessment of right ventricular function: current clinical practice. Int J Cardiovasc Imaging. 2019;35(1):49–56.

65. Soliman-Aboumarie H, Joshi SS, Cameli M, Michalski B, Manka R, Haugaa K, Demirkiran A, Podlesnikar T, Jurcut R, Muraru D, Badano LP, Dweck MR. EACVI survey on the multi-modality imaging assessment of the right heart. Eur Heart J Cardiovasc Imaging. 2022;23(11):1417–1422.

66. Lang RM, Addetia K, Narang A, Mor-Avi V. 3-Dimensional Echocardiography: Latest Developments and Future Directions. JACC Cardiovasc Imaging. 2018;11(12):1854–1878.

67. Kalam K, Otahal P, Marwick TH. Prognostic implications of global LV dysfunction: a systematic review and meta-analysis of global longitudinal strain and ejection fraction. Heart. 2014;100(21):1673–1680.

68. Stokke TM, Hasselberg NE, Smedsrud MK, Sarvari SI, Haugaa KH, Smiseth OA, Edvardsen T, Remme EW. Geometry as a Confounder When Assessing Ventricular Systolic Function. JACC. 2017;70(8):942–954.

69. Kovács A, Tapolyai M, Celeng C, Gara E, Faludi M, Berta K, Apor A, Nagy A, Tislér A, Merkely B. Impact of hemodialysis, left ventricular mass and FGF-23 on myocardial mechanics in end-stage renal disease: a three-dimensional speckle tracking study. Int J Cardiovasc Imaging. 2014;30(7):1331–1337.

70. Lee H-F, Hsu L-A, Chan Y-H, Wang C-L, Chang C-J, Kuo C-T. Prognostic value of global left ventricular strain for conservatively treated patients with symptomatic aortic stenosis. J Cardiol. 2013;62(5):301–306.

71. Buckberg G, Hoffman JIE. Right ventricular architecture responsible for mechanical performance: Unifying role of ventricular septum. J Thorac Cardiovasc Surg. 2014;148(6):3166–3171.e3164.

72. Friedberg Mark K. Imaging Right-Left Ventricular Interactions. JACC Cardiovasc Imaging. 2018;11(5):755–771.

73. Swift AJ, Rajaram S, Capener D, Elliot C, Condliffe R, Wild JM, Kiely DG. Longitudinal and Transverse Right Ventricular Function in Pulmonary Hypertension: Cardiovascular Magnetic Resonance Imaging Study from the ASPIRE Registry. Pulm Circ. 2015;5(3):557–564.

74. Jategaonkar SR, Scholtz W, Butz T, Bogunovic N, Faber L, Horstkotte D. Two-dimensional strain and strain rate imaging of the right ventricle in adult patients before and after percutaneous closure of atrial septal defects. Eur J Echocardiogr. 2009;10(4):499–502.

75. Raina A, Vaidya A, Gertz ZM, Susan C, Forfia PR. Marked changes in right ventricular contractile pattern after cardiothoracic surgery: Implications for post-surgical assessment of right ventricular function. J Heart Lung Transplant. 2013;32(8):777–783.

76. Kitano T, Kovács A, Nabeshima Y, Tokodi M, Fábián A, Lakatos BK, Takeuchi M. Prognostic Value of Right Ventricular Strains Using Novel Three-Dimensional Analytical Software in Patients With Cardiac Disease. Front Cardiovasc Med. 2022;Volume 9 - 2022:837584.

77. Ladányi Z, Lakatos BK, Clement A, Tomaselli M, Fábián A, Radu N, Turschl TK, Ferencz A, Merkely B, Surkova E, Kovács A, Muraru D, Badano LP. Mechanical Adaptation of the Right Ventricle to Secondary Tricuspid Regurgitation and Its Association With Patient Outcomes. J Am Soc Echocardiogr. 2025;38(7):601–612.

78. Keller M, Fábián A, Bandini A, Szijártó Á, Tősér Z, Merkely B, Heller T, Dürr MM, Rosenberger P, Kovács A, Magunia H. Impact of the right ventricular mechanical pattern assessed by three-dimensional echocardiography on adverse outcomes following cardiac surgery. Sci Rep. 2025;15(1):5623.

79. Brener MI, Masoumi A, Ng VG, Tello K, Bastos MB, Cornwell WK, 3rd, Hsu S, Tedford RJ, Lurz P, Rommel KP, Kresoja KP, Nagueh SF, Kanwar MK, Kapur NK, Hiremath G, Sarraf M, Van Den Enden AJM, Van Mieghem NM, Heerdt PM, Hahn RT, Kodali SK, Sayer GT, Uriel N, Burkhoff D. Invasive Right Ventricular Pressure-Volume Analysis: Basic Principles, Clinical Applications, and Practical Recommendations. Circ Heart Fail. 2022;15(1):e009101.

80. Ruppert M, Lakatos BK, Braun S, Tokodi M, Karime C, Olah A, Sayour AA, Hizoh I, Barta BA, Merkely B, Kovacs A, Radovits T. Longitudinal Strain Reflects Ventriculoarterial Coupling Rather Than Mere Contractility in Rat Models of Hemodynamic Overload-Induced Heart Failure. J Am Soc Echocardiogr. 2020;33(10):1264–1275 e1264.

9. Bibliography of the candidate's publications

9.1. Bibliography related to the present thesis

1. **Máté Tolvaj**, Márton Tokodi, Bálint Károly Lakatos, Alexandra Fábián, Adrienn Ujvári, Fjolla Zhubi Bakija, Zsuzsanna Ladányi, Zsófia Tarcza, Béla Merkely, Attila Kovács (2021) Added predictive value of right ventricular ejection fraction compared with conventional echocardiographic measurements in patients who underwent diverse cardiovascular procedures.
   IMAGING, doi:10.1556/1647.2021.00049
   IF: **0**

2. **Máté Tolvaj***, Attila Kovács*, Noela Radu, Andrea Cascella, Denisa Muraru, Bálint Lakatos, Alexandra Fábián, Márton Tokodi, Michele Tomaselli, Mara Gavazzoni, Francesco Perelli, Béla Merkely, Luigi P. Badano, Elena Surkova (2024) Significant Disagreement Between Conventional Parameters and 3D Echocardiography-Derived Ejection Fraction in the Detection of Right Ventricular Systolic Dysfunction and Its Association With Outcomes.
   J Am Soc Echocardiogr, doi: 10.1016/j.echo.2024.04.005.
   IF: **6.0**
   *Máté Tolvaj and Attila Kovács are joint first authors.

3. **Máté Tolvaj**, Alexandra Fábián, Márton Tokodi, Bálint Lakatos, Alexandra Assabiny, Zsuzsanna Ladányi, Kai Shiida, Andrea Ferencz, Walter Schwertner, Boglárka Veres, Annamária Kosztin, Ádám Szijártó, Balázs Sax, Béla Merkely, Attila Kovács (2023) There is more than just longitudinal strain: Prognostic significance of biventricular circumferential mechanics.
   Front Cardiovasc Med, doi: 10.3389/fcvm.2023.1082725.
   IF: **2.8**

9.2. Bibliography not related to the present thesis

1. Márton Tokodi, Bálint Magyar, András Soós, Masaaki Takeuchi, **Máté Tolvaj**, Bálint Károly Lakatos, Tetsuji Kitano, Yosuke Nabeshima, Alexandra Fábián, Mark Bence Szigeti, András Horváth, Béla Merkely, Attila Kovács (2023) Deep Learning-Based Prediction of Right Ventricular Ejection Fraction Using 2D Echocardiograms.
   JACC Cardiovasc Imaging doi: 10.1016/j.jcmg.2023.02.017.
   IF: **12.8**

2. Ádám Szijártó, Alexandra Fábián, Bálint Károly Lakatos, **Máté Tolvaj**, Béla Merkely, Attila Kovács, Márton Tokodi (2023) A machine learning framework for performing binary classification on tabular biomedical data.
   IMAGING, doi:10.1556/1647.2023.00109
   IF: **0.7**

3. Borbála Edvi, Alexandra Assabiny, Tímea Teszák, **Máté Tolvaj**, Alexandra Fábián, István Hartyánszky, Miklós Pólos, Bálint Károly Lakatos, Hajnalka Vágó, Balázs Sax, Béla Merkely, Attila Kovács (2024) Trajectory of Diastolic Function after Heart Transplantation as Assessed by Left Atrial Deformation Analysis.
   Diagnostics, doi: 10.3390/diagnostics14111136.
   IF: **3.3**

4. Zsuzsanna Ladányi, Abdalla Eltayeb, Alexandra Fábián, Adrienn Ujvári, **Máté Tolvaj**, Márton Tokodi, Kashif Anwar Choudhary, Attila Kovács, Béla Merkely, Olga Vriz, Bálint Károly Lakatos (2024) The effects of mitral stenosis on right ventricular mechanics assessed by three-dimensional echocardiography.
   Sci Rep., doi: 10.1038/s41598-024-68126-y.
   IF: **3.9**

5. **Máté Tolvaj**, Fjolla Zhubi Bakija, Alexandra Fábián, Andrea Ferencz, Bálint Lakatos, Zsuzsanna Ladányi, Ádám Szijártó, Edvi Borbála, Loretta Kiss, Zsolt Szelid, Pál Soós, Béla Merkely, Zsolt Bagyura, Márton Tokodi, Attila Kovács (2025) Integrating Left Atrial Reservoir Strain Into the First-Line Assessment of Diastolic Function: Prognostic Implications in a Community-Based Cohort With Normal Left Ventricular Systolic Function.
   J Am Soc Echocardiogr, doi: 10.1016/j.echo.2025.03.012
   IF (2024): **6.0**

6. Ádám Szijártó, Béla Merkely, Attila Kovács, Márton Tokodi on behalf of the **QUEST-EF Investigators** (2025) Deep learning-enabled echocardiographic assessment of biventricular ejection fractions: the dual-task QUEST-EF model.
   Eur. Heart J. Cardiovasc. Imaging., doi: 10.1093/ehjci/jeaf147

7. Fjolla Zhubi Bakija, **Máté Tolvaj**, Ádám Szijártó, Márton Tokodi, Andrea Ferencz, Bálint Károly Lakatos, Zsuzsanna Ladányi, Loretta Kiss, Zsolt Szelid, Pál Soós, Béla Merkely, Zsolt Bagyura, Attila Kovács, Alexandra Fábián (2025) Long-term prognostic value of myocardial work analysis across obesity stages: insights from a community-based study
   Int. J. Obes., doi: 10.1038/s41366-025-01863-w
   IF (2024): **3.8**

10. Acknowledgements

I am deeply grateful to the people who helped and supported me during my doctoral studies. Without them, I would not have been able to conduct my research and prepare this thesis.

First and foremost, I am profoundly thankful to my supervisor, Dr. Attila Kovács, whom I greatly respect and admire for his academic experience, knowledge, and personal attributes. Dr. Kovács always supported and motivated me, not only providing opportunities but also his guidance and advice whenever I needed it. Thank you for guiding and supporting me through every step of my academic path. Without hesitation, I can say I could not have wished for a better mentor.

I would like to express my deepest gratitude to Prof. Dr. Béla Merkely for providing exceptional professional guidance and outstanding opportunities within a highly stimulating scientific environment, all of which were instrumental to the successful completion of my doctoral research.

I would also like to extend my special thanks to my student-research co-supervisors, Dr. Márton Tokodi and Dr. Alexandra Fábián, who taught me the fundamentals (and beyond) of statistical analysis and presentation, never sparing their time or effort whenever their expertise was needed. I am likewise grateful to the other members of the research group I have been part of — Dr. Bálint Lakatos, Dr. Adrienn Ujvári, Dr. Zsuzsanna Ladányi, Ádám Szijártó, Dr. Andrea Ferencz, and Dr. Tímea Turschl — who welcomed me into the group and, in addition to their support and kindness, offered their friendship, for which I am deeply thankful.

I would like to express my sincere gratitude to all co-authors and colleagues who have contributed to the research presented in this thesis.

I wish to express my heartfelt gratitude to my parents for their constant support in all aspects of my life. Their dedication, values, and tireless efforts throughout my upbringing have shaped both my character and my persistence, laying the foundation for my achievements. I am deeply thankful for their encouragement, love, and the sacrifices they made to help me become the person I am today.

Last, but not least, I would like to offer my sincere gratitude to my grandmother. Her kindness and support created a stable and enabling environment that allowed me to focus on my medical studies. I am profoundly grateful for her selflessness and love, which have been a constant source of strength and comfort during the challenges of my academic pursuits.